U. S. ARMY

Technical Memorandum 26-70

VISUAL DETECTION OF ILLUMINATING SURFACES

Richard T. Mauriganis

October 1970

AMCMS Code 5024.11.81900

HUMAN ENGINEERING LABORATORIES

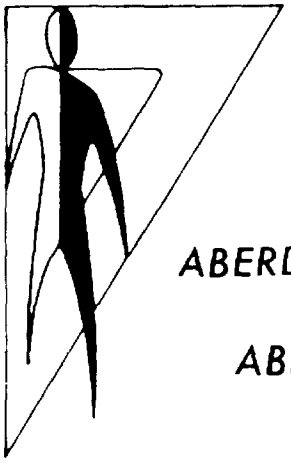

ABERDEEN RESEARCH & DEVELOPMENT CENTER

ABERDEEN PROVING GROUND, MARYLAND

Destroy this report when no longer needed
Do not return it to the originator

The findings in this report are not to be construed as an official Department of the Army position unless so designated by other authorized documents

Use of trade names in this report does not constitute an official endorsement or approval of the use of such commercial products

AMCMS Code 502F.11.81900 Technical Memorandum 26-70

VISUAL DETECTION OF ILLUMINATING SURFACES

Richard T. Maruyama

TECHNICAL LIBRARY
ABERDEEN PROVING GROUND, MD.
STEAP-TL

October 1970

APPROVED: JOHN D. WEISZ
Director
Human Engineering Laboratories

HUMAN ENGINEERING LABORATORIES
U. S. Army Aberdeen Research & Development Center
Aberdeen Proving Ground, Maryland

This document has been approved for public release and sale; its distribution is unlimited.

FOREWORD

The author wishes to thank Dr. David L. MacAdam, Editor of the Journal of the Optical Society of America, for granting permission to publish six graphs and two tables that appeared in the journal. The six graphs were presented by E. S. Lamar, S. Hecht, C. D. Hendley and S. Shlaer in their report, "Size, Shape and Contrast in Detection of Targets by Daylight Vision I. Data and Analytical Description." The two tables were taken from S. Q. Duntley's report, "The Reduction of Apparent Contrast by the Atmosphere."

ABSTRACT

Determining the requirements of helicopter lighting requires selecting the major factors that contribute to the lighting power of a surface light source. Since the light source must be functional, sky brightness, atmospheric attenuation, and other characteristics of light sources such as size, shape and angular velocity must be studied. This report presents a model that looks at each of these variables separately. More investigation is needed in the field of search time to improve the reliability of the model for given background luminances.

The necessary light output for an area light source can be determined by methods described; in addition the required boundary range for a surface light source can be computed for almost all conditions.

CONTENTS

ABSTRACT iii

INTRODUCTION 1

CONSIDERATION OF VISUAL TARGET AREA 2

SHAPE OF TARGETS AND CONTRAST REQUIREMENTS 5

ATTENUATION AND SCATTER 21

TIME AS A FACTOR OF INCREASING THE PROBABILITY OF DETECTION. . 37

SUMMARY 60

REFERENCES 61

APPENDIX 63

FIGURES

1. Angular Subtense of 20 Square Inch EL Panel in Equivalent Circular Surface 3

2. Difference in 50% Probability Contrast Limens with 1:1 and 100:1 Length to Width Ratios with Background Brightness 10^{-5} Foot-Lamberts 6

3. Useful Flux and Its Relation to Target Perimeter with Background Brightness 10^{-1} Foot-Lamberts 8

4. Useful Flux and Its Relation to Target Perimeter with Background Brightness 10^{-3} Foot-Lamberts 9

5. Useful Flux and Its Relation to Target Perimeter with Background Brightness 10^{-5} Foot-Lamberts 10

6. Useful Flux and Its Relation to Target Perimeter with Background Brightness, From Reference 9 11

7. Relation Between Threshold Contrast and Angular Area of Target-Foveal Vision From Reference 9 12

8. Relation Between Total Flux and Angular Length of Target-Foveal Vision From Reference 9 14

9. Relation Between Total Flux and Angular Length of Target Points Calculated From Reference 9 Data and Plotted by Inspection (background brightness 1 x 10^{-1} foot-lamberts) 15

10. Relation Between Total Flux and Angular Length of Target Points Calculated From Reference 9 Data and Plotted by Inspection (background brightness 1 x 10^{-3} foot-lamberts) 16

11. Relation Between Total Flux and Angular Length of Target Points Calculated From Reference 9 Data and Plotted by Inspection (background brightness 1 x 10^{-5} foot-lamberts) 17

12. Target Assumed to be Circular (shows the useful flux for the case of 10^{-3} foot-lamberts background) 19

13. Relation Between Threshold Contrast and Angular Area for Rectangular Targets with Different Length to Width Ratios (background brightness 10^{-1} foot-lamberts) 22

14. Relation Between Threshold Contrast and Angular Area for Rectangular Targets with Different Length to Width Ratios (background brightness 10^{-3} foot-lamberts) 23

15. Relation Between Threshold Contrast and Angular Area for Rectangular Targets with Different Length to Width Ratios (background brightness 10^{-5} foot-lamberts) 24

16. Illustrating the Two Constant Theory 25

17. For the General Case of Downward Visibility for a Target Not on the Ground 32

18. Relation Between Threshold Requirement for EL-Panel (slant range) and Distance (looking downward position-10^{-3} foot-lamberts) 38

19. Relation Between Threshold Requirement for EL-Panel (slant range) and Distance (horizontal position-10^{-3} foot-lamberts) . . 39

20. Relation Between Threshold Requirement for EL-Panel (slant range) and Distance (looking upward position-10^{-3} foot-lamberts) . 40

21. Relation Between Threshold Requirement for EL-Panel (slant range) and Distance (looking downward position-10^{-4} foot-lamberts) 41

22. Relation Between Threshold Requirement for EL-Panel (slant range) and Distance (horizontal position - 10^{-4} foot-lamberts) 42

23. Relation Between Threshold Requirement for EL-Panel (slant range) and Distance (looking upward position - 10^{-4} foot-lamberts) 43

24. Relation Between Threshold Requirement for EL-Panel (slant range) and Distance (looking downward position - 10^{-5} foot-lamberts) . . . 44

25. Relation Between Threshold Requirement for EL-Panel (slant range) and Distance (horizontal position - 10^{-5} foot-lamberts) 45

26. Relation Between Threshold Requirement for EL-Panel (slant range) and Distance (looking upward position - 10^{-5} foot-lamberts) 46

27. Target Moving in a Straight Path at Constant Velocity and Constant Altitude 47

28. Relation Between Linear Search Area (A), Contrast ($\Delta I/I$), and Delay (Search) Time (Δt) 50

29. Time to Detection Vs Search Area; Grand Average (Source: Krendel & Wolinsky) 51

30. Average Probability Curve for 450,000 Sample Population 54

31. Detection Probability for EL-Panel with Brightness 4.936×10^{-3} . . 56

TABLES

1. Some of the Liminal Contrast of Circular Targets by Hardy . . . 2

2. Blackwell's Reported Data: Liminal Contrast Ratios Associated with Shapes 7

3. Data Used to Calculate Constants k and C 20

4. Sky-Ground Ratio 31

5. Relative Density of Air Due to Altitude 35

6. Relationship Between Area (A), Contrast $(\Delta I/I)_L$ and Delay Time (ΔT) 49

7. Detection Probability Levels Required for Fixed Light Sources . . 52

8. Probability Levels for an Approaching Target of $.4936 \times 10^{-2}$ Foot-Lamberts at 1,063 Feet 55

9. Time Required to Detect the Approaching Target in Figure 15 . . . 57

VISUAL DETECTION OF ILLUMINATED SURFACES [1]

INTRODUCTION

This study was initiated in response to the expressed need for better formation flight lighting for U. S. Army helicopters. Electroluminescent (EL) panels and rotor tip lights were under active consideration as potential improvements over the navigation/position lights currently used in formation. Studies by the U. S. Army Electronics Command Avionics Laboratory and the U. S. Army Limited War Laboratory indicated interest in electroluminescent panel lights and both incandescent and self-luminous rotor tip lights.

To guarantee signal characteristics under a wide range of operational conditions, it was necessary to study a large number of functional relationships. These would permit prediction of lighting requirements based on the following variables:

a. Geometry of the target in respect to the observer.

b. Atmospheric attenuation and scattering.

c. Uniform and non-uniform background luminance.

d. Exposure time of target to the observer in the field.

e. Size of target.

f. Shape of target.

g. Angular velocity (minutes per second) of target source in the field.

Throughout this report, it will be assumed that altitude, velocity and terrain are constant for any given problem.

[1]This study was part of a program funded by Avionics Laboratory, U. S. Army Electronics Command, Fort Monmouth, New Jersey.

CONSIDERATION OF VISUAL TARGET AREA

Threshold levels for visual detection of light sources were provided by Hardy (6) for targets subtending given minutes of visual arc and given background luminance conditions. Data used here were abstracted from the World War II visibility studies carried out by the Tiffany Foundation under a contract with the Office of Scientific Research and Development and reported in Hardy's July 1963 report titled, "Visibility Data and the Use of Optical Aids" (Table 1).

TABLE 1

Some of the Liminal Contrast of Circular Targets by Hardy

Angular Subtense of Target (Min.)	Liminal Contrast (Foot-Lamberts)								
	1,000	100	10	1	10^{-1}	10^{-2}	10^{-3}	10^{-4}	10^{-5}
20.43	.00335	.00335	.00357	.00498	.0113	.0414	.211	.676	2.27
7.430	.00562	.00605	.00787	.0126	.0309	.133	.995	4.20	16.1
6.290	.00667	.00745	.0100	.0166	.0413	0.175	1.38	5.82	22.6
1.988	.0444	.0566	.0838	.150	.376	1.61	13.6	58.3	225.
1.360	0.0881	0.116	0.175	0.312	0.785	3.45	29.0	125.	480.
1.292	0.0966	0.128	0.193	0.345	0.868	3.82	32.2	138.	535.
0.8170	0.225	0.306	0.466	0.841	2.14	9.44	79.4		1330.

Using Hardy's contrast thresholds for circular targets, a number of computer calculations were performed in order to determine the light values required under various conditions of range, shape, size, attenuation and scatter. Since Hardy's threshold values apply only to targets subtending the same shapes and visual angles, application of Hardy's threshold levels to other targets involves a transformation to equivalent shapes and sizes.

Problems in shape transformations will be discussed in the next section. However, in general, rectangles with small length-to-width ratios such as squares, or the 2-inch by 10-inch electroluminescent panels, can be transformed to equivalent circular areas. The curve for angular subtense of the 2 x 10-inch electroluminescant panels was derived through the following calculations (Fig. 1):

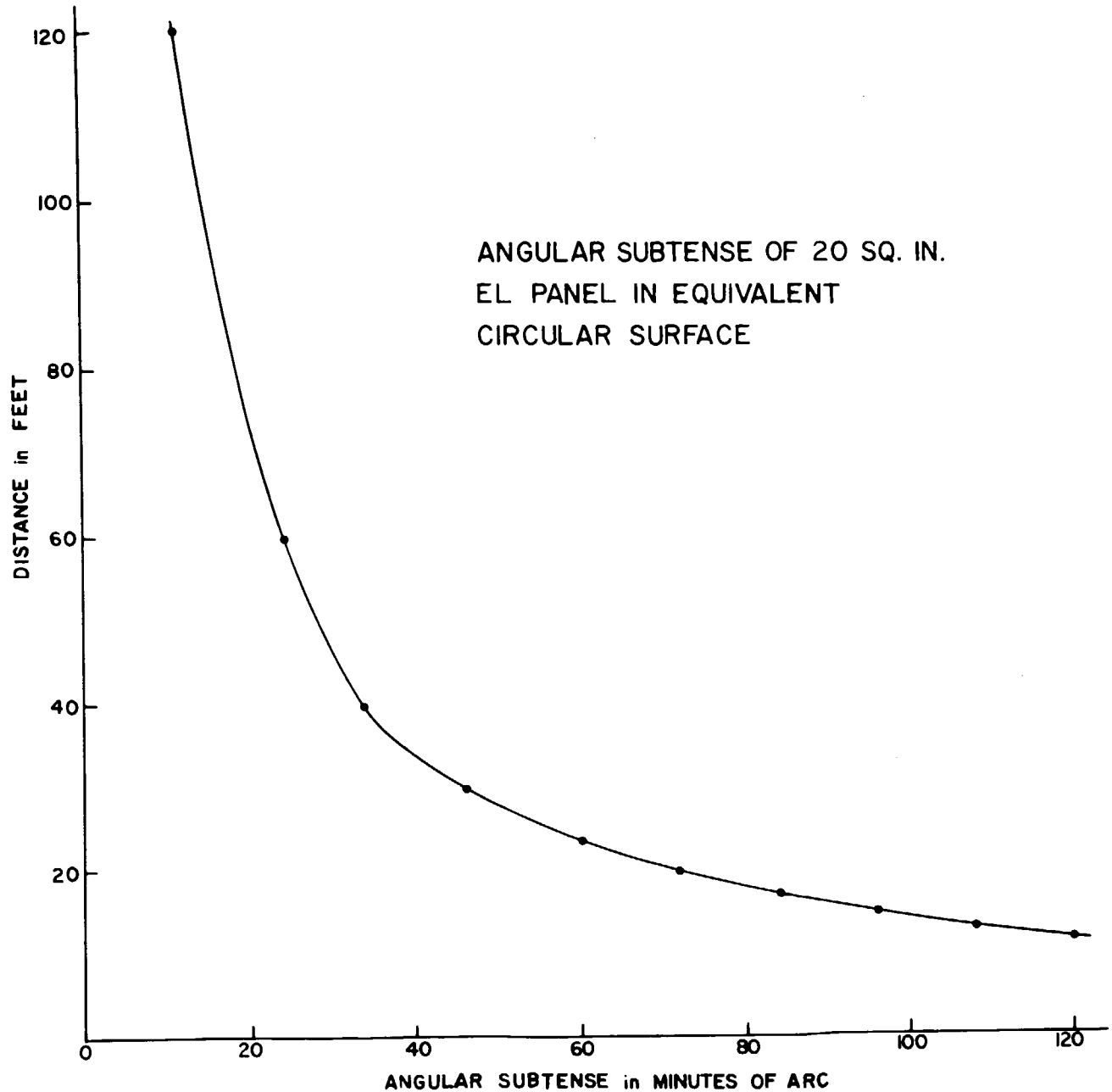

Fig. 1. ANGULAR SUBTENSE OF 20 SQUARE INCH EL PANEL IN EQUIVALENT CIRCULAR SURFACE

$\pi r^2 = \frac{X}{144}$ (converting target area, X, in square inches to square feet)

$r = \sqrt{\frac{X}{144\pi}}$ (radius in feet of an equivalent circular target to the 2 x 10 inch electroluminescent panel)

$\frac{r}{d} = \text{Tan}\left(\frac{\theta}{2}\right)$ (where r = radius of equivalent circle and d = distance from observer)

$d = \frac{r}{\text{Tan}\left(\frac{\theta}{2}\right)}$ (d = distance at which the electroluminescent panel will subtend θ minutes of arc)

For the case of the electroluminescent panels, 2 x 10 inches, at distances 100 feet or more, we are concerned with thresholds of less than 15 minutes of visual arc. Hence, for visibility or detection at flight separations beyond 200 feet, we can examine visual thresholds of surfaces subtending less than 7.2276 minutes of visual arc for the 2 x 10 inches electroluminescent panel.

$r = .21026$ (radius of the 2 x 10 inch electroluminescent panels x target in feet)

$\theta = 2\ \text{Tan}^{-1}\left(\frac{r}{200}\right)$

$\theta = 2\ \text{Tan}^{-1}\ (.00105131)$

$\theta = 7.2276$ minutes of arc (θ is the angle the target subtense at a distance of 200 feet)

Therefore, Hardy's contrast thresholds for less than 7.23 minutes of visual arc were used for ranges (distances) of 200 feet or more.

SHAPE OF TARGETS AND CONTRAST REQUIREMENTS

The threshold contrasts of targets with sides in the ratios of 1:1 and 100:1 will differ depending upon the ratios; the larger the length to width ratio, the greater the contrast ratio required, except for surfaces subtending extremely small angles. Blackwell's Tiffany Foundation studies done during World War II reported on this subject. His results are illustrated in Figure 2 showing the different contrast requirements for two targets against background luminance of 1×10^{-5} foot lamberts. Table 2 shows the excerpted data that Blackwell experimentally produced.

Lamar (9) made the assumption that contrast is not judged over an entire target area, but only across its boundary. Lamar worked with targets ranging from 0.5 to 800.0 square minutes in area. The following calculation is based on contrast between the boundary of the target and the boundary of the background, where Blackwell's and Hardy's data were used for the calculations. Lamar's data was obtained from the records of one dozen subjects (under 30 years of age, with 20/20 vision or better). The data used to compute luminal contrast ($\Delta I/L_t$) represent accurately the threshold levels of the human eye for different background luminances and sizes.

Useful flux is defined as the light from an area just inside the perimeter of the target; the width of this perimeter varies according to the background luminance. Figures 3, 4, and 5 show the relationship between useful flux and target perimeters under low light level conditions.

The width of the perimeter band is determined by examining Hardy's data. There is a critical width at which the total flux slopes upward as the area of the target increases. This upward slope implies that as the area increases beyond a critical width, the total light flux increases in proportion to the increase of the added area of the target. Hence the flux contributed by points inside the critical band will not add to the visibility of the target. Since this upward slope occurs at a fixed width depending upon the background luminance, it is reasonable to assume that this will occur for any extended target shape. That is, the total flux will not be totally useful beyond a critical width inside the edge of the perimeter, and this critical width implies that detection will occur because of the contrast on the perimeter.

These curves (Figs. 3, 4 and 5) have the same shape as those by Lamar (Fig. 6), which impiles that Lamar's rule may hold under scotopic as well as photopic background luminances. Examination of Figure 7 (Lamar) suggests that there is little difference between curves for asymmetry quotients 2 and 7. For small asymmetry the ratio of length to width is relatively unimportant, the variable of major importance is area, not shape of target. However, for ratios above 10 or 20 the target shape becomes important, and the contrast threshold rises as the target ratio increases.

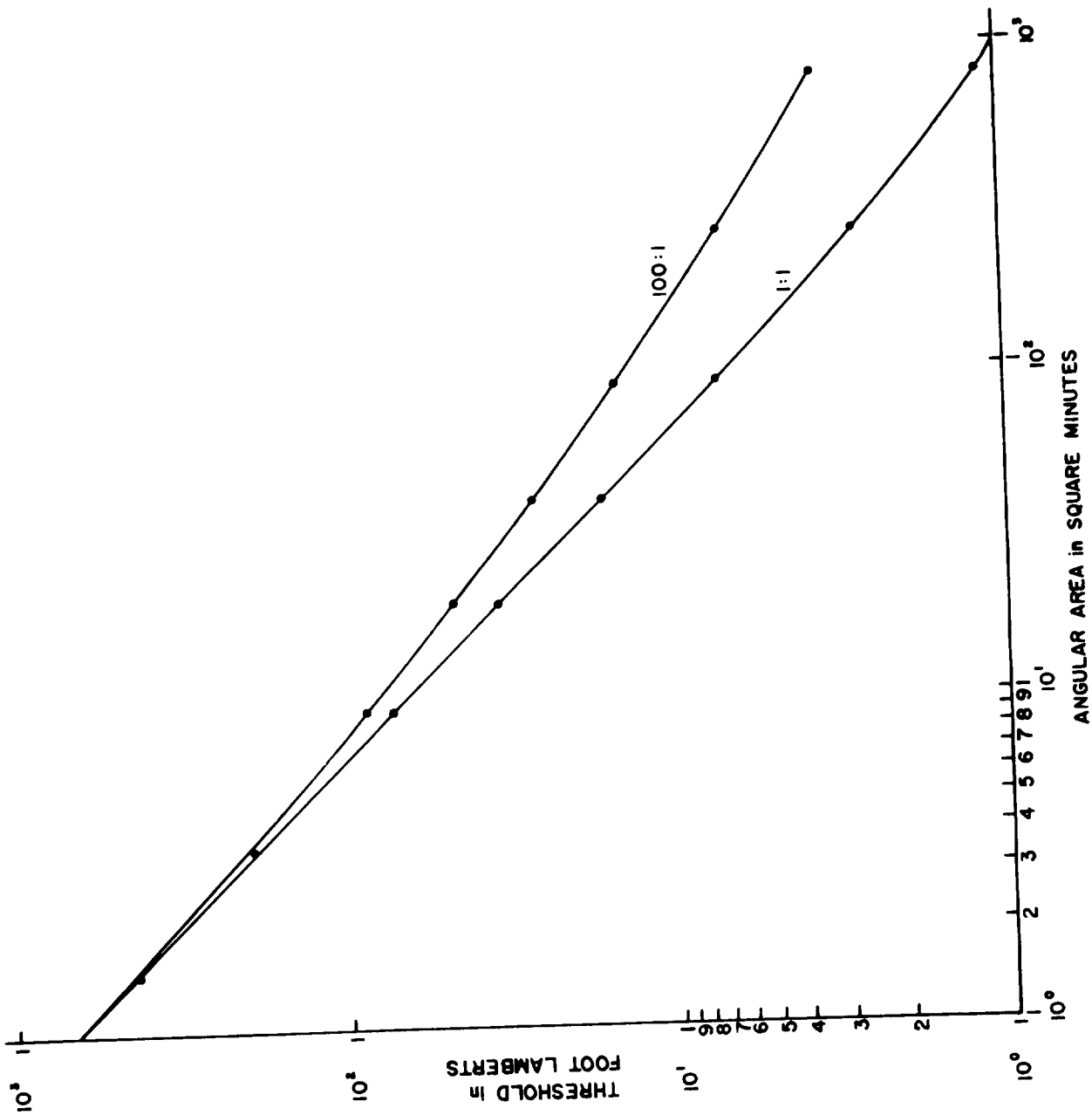

Fig. 2. DIFFERENCE IN 50% PROBABILITY CONTRAST LIMENS WITH 1:1 AND 100:1 LENGTH TO WIDTH RATIOS WITH BACKGROUND BRIGHTNESS 10^{-5} FOOT-LAMBERTS

TABLE 2

Blackwell's Reported Data: Liminal Contrast Ratios Associated With Shapes

Shape	Dimensions in Minutes Area/Diameter	Liminal Contrast	Background (Foot-Lamberts)
Circle	(1,734.909) 47.	.764	10^{-5}
Square	(1,751.3) 41.5 x 42.2	.804	10^{-5}
Rectangle 100:1	(1,760.0) 400 x 4.4	1.97	10^{-5}
Circle	(1,734.909) 47.	.00541	10
Square	(1,751.30) 41.5 x 42.2	.00374	10
Rectangle 100:1	(1,760.0) 400 x 4.4	.00589	10
Rectangle 5:1	(6.2422) 5.29 x 1.18	.0560	10
Rectangle 4:1	(1,728.48) 83.1 x 20.8	.00512	10
Rectangle 10:1	(48.4) 22.0 x 2.2	.0200	10
Rectangle 100:1	(46.134) 69.9 x .660	.0454	10

Liminal Contrast Ratios

Visual Angle (Minutes)	Circle or Square	100:1 Rectangle	
129.2	0.259		
64.60	0.485		Adaptation Brightness
32.30	1.12	3.53	10^{-5} foot-lamberts
18.46	2.71	7.31	
10.77	7.73	15.1	
7.178	17.3	27.5	
4.969	36.1	48.8	
3.400	77.4	89.5	
3.076	94.1	107.0	
2.153	192.0	200.0	
1.436	432.0	432.0	

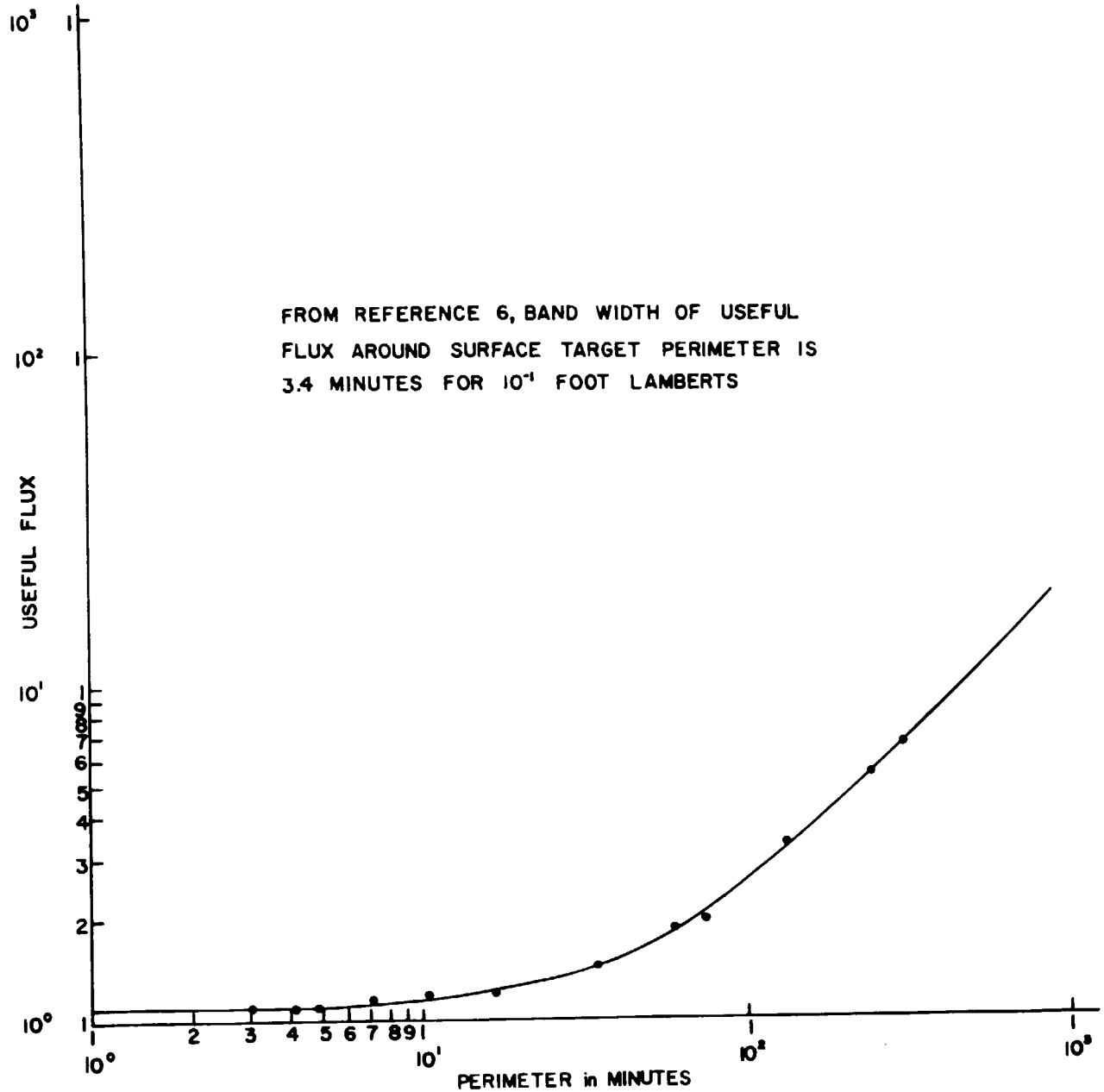

Fig. 3. USEFUL FLUX AND ITS RELATION TO TARGET PERIMETER WITH BACKGROUND BRIGHTNESS 10^{-1} FOOT-LAMBERTS

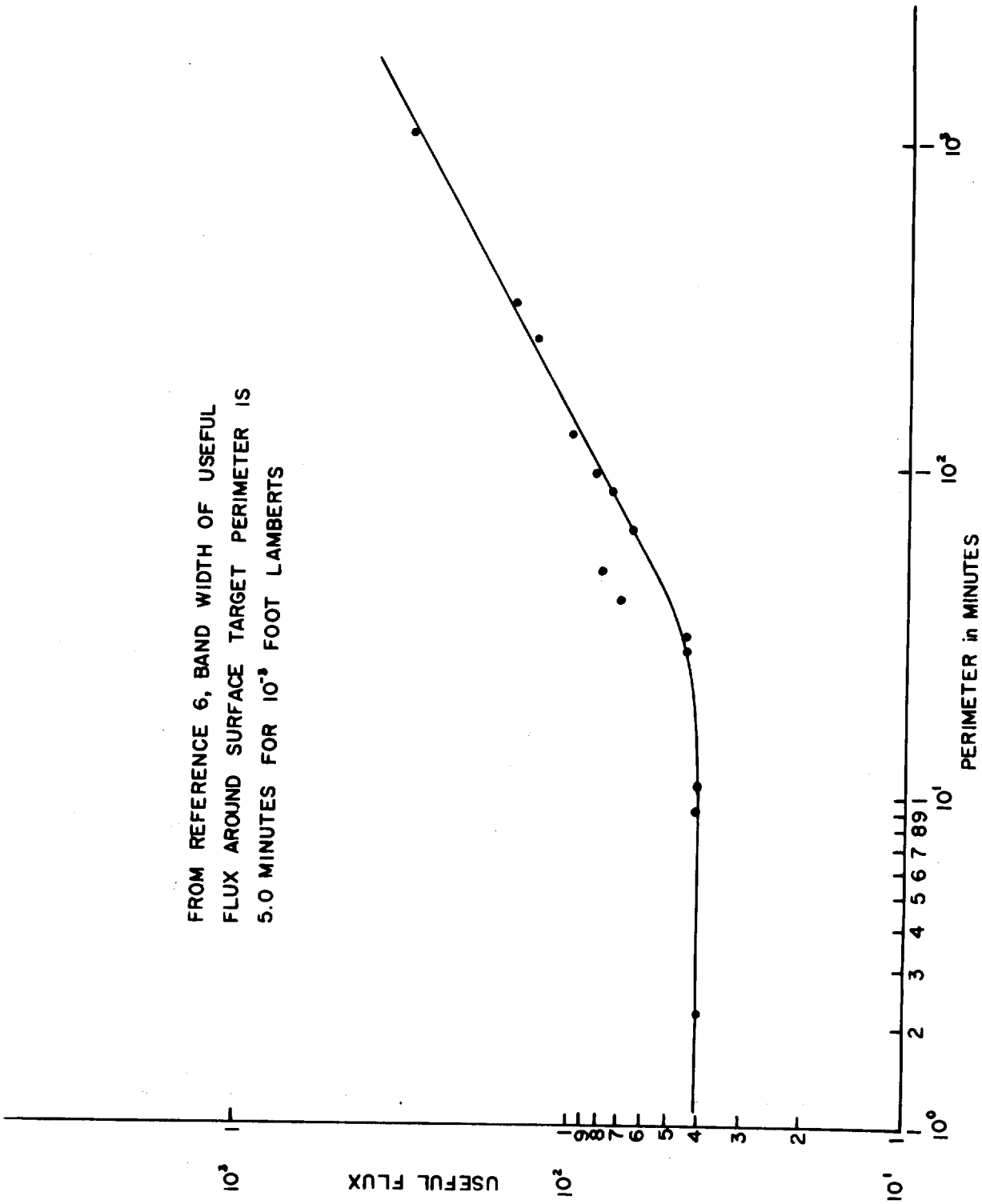

Fig. 4. USEFUL FLUX AND ITS RELATION TO TARGET PERIMETER WITH BACKGROUND BRIGHTNESS 10^{-3} FOOT-LAMBERTS

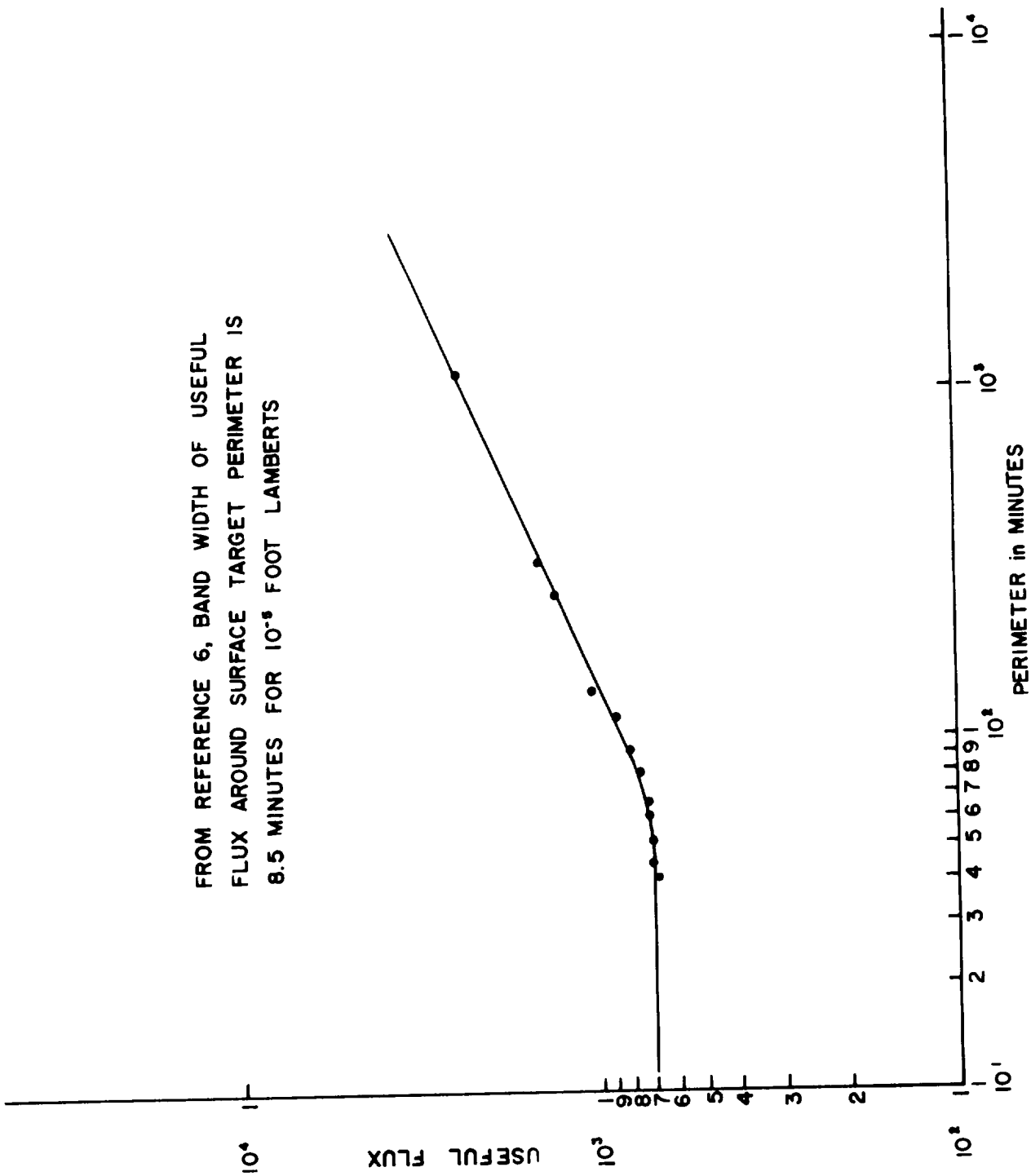

Fig. 5. USEFUL FLUX AND ITS RELATION TO TARGET PERIMETER WITH BACKGROUND BRIGHTNESS 10^{-5} FOOT-LAMBERTS

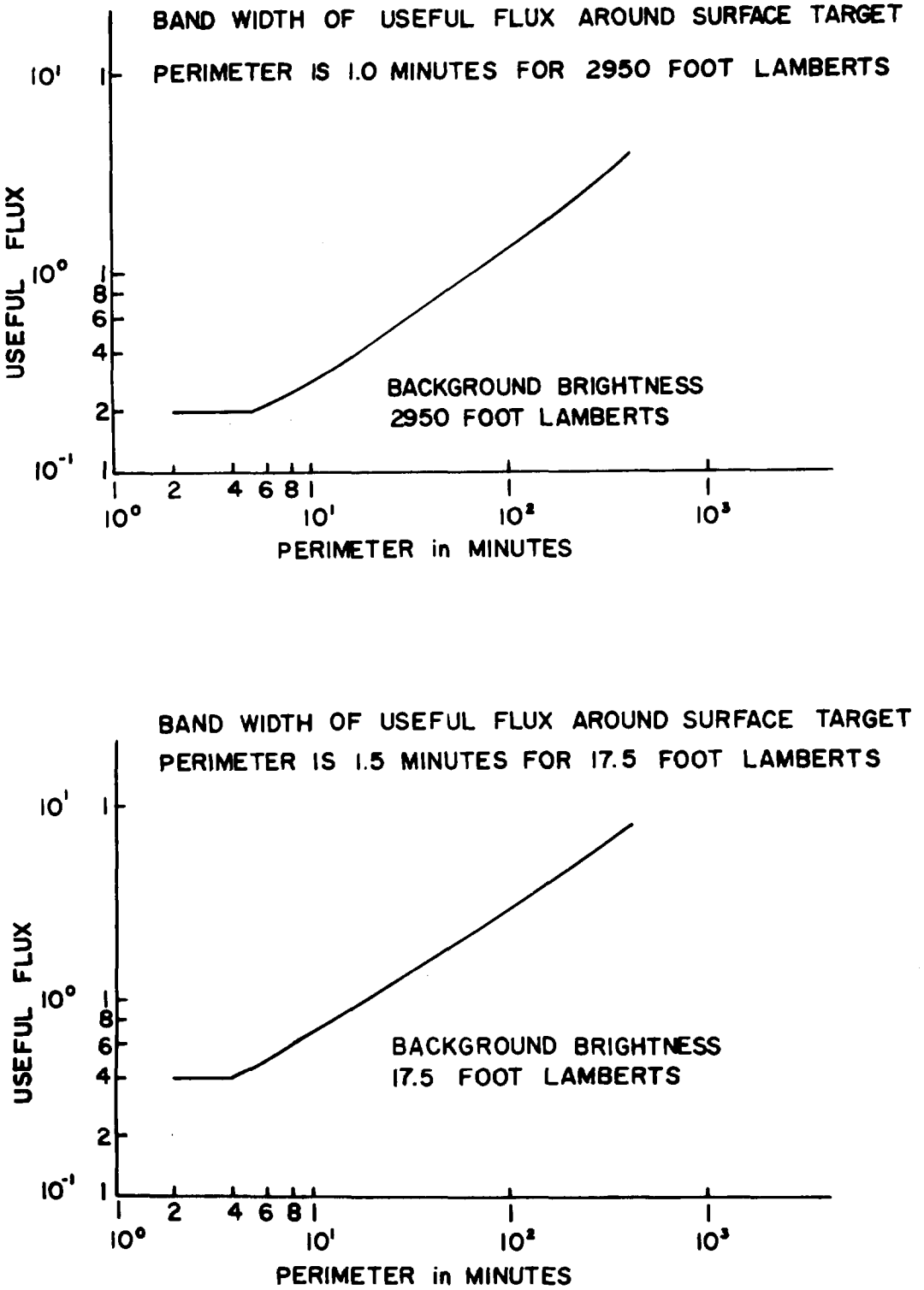

Fig. 6. USEFUL FLUX AND ITS RELATION TO TARGET PERIMETER, FROM REFERENCE 9

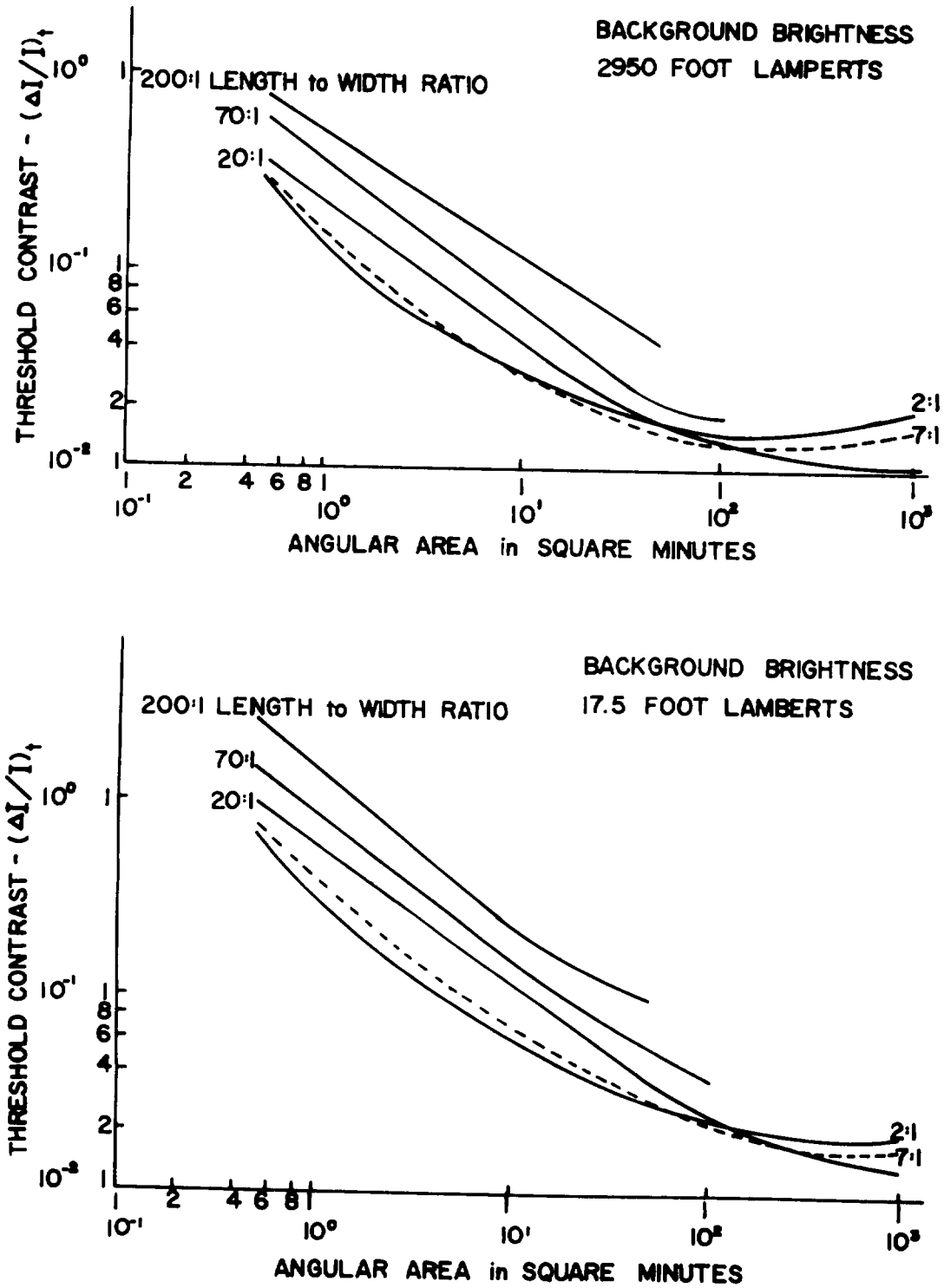

Fig. 7. RELATION BETWEEN THRESHOLD CONTRAST AND ANGULAR AREA OF TARGET-FOVEAL VISION FROM REFERENCE 9

The concept of useful flux that Lamar presented indicates that the two quantities which determine a target's detectability is the amount of contrast across a boundary and the perimeter size. The formula is:

$$\left(\frac{\Delta I}{I}\right)_t = C R^k / A_1 \qquad (1)$$

where (C) is a constant, (R) is the perimeter of the target in minutes of arc, (A_1) is the area of useful flux, and (k) is the constant for background which determines the slope of the useful flux curve.

This appears to be a way of integrating some of the theoretical modifications of Ricco's Law as applied to targets of intermediate size (Graham, Chapter 7 by Bartlett). Ricco's Law states that the product of area and luminance is constant for threshold ($AL = k$). This law holds nicely for small targets, generally targets less than one minute and approaching point light sources in size. Ricco's Law holds also for larger targets, up to 10 to 14 minutes in diameter, if the background is very dark, permitting targets at threshold to be less bright. This law is consistent with the useful flux concept in that all the flux is useful in these cases. However, as the target becomes extended, Ricco's Law does not apply, and various modifications have been suggested. For example, Piper's equation gives an approximate description of the situation for intermediate sizes. (The product of the square root of area and luminance is constant, $\sqrt{A}L = k$. However, neither Ricco's Law nor Piper's equation will correctly describe targets which deviate from the point symmetry of a square or circle. Lamar's formula better indicates the efficiency of the light flux available throughout this range of targets, and can be applied as well to extended targets or targets of assymetrical shape. Graham, Brown and Mote (Graham, Chapter 7 by Bartlett) have developed a theory which applies to targets throughout the range of sizes except for the very small targets, but this theory is more complicated in application and is also limited to symmetrical targets. Lamar's formula is easier to apply and can be extended to targets as large as 800 minutes in area. However, it is inapplicable to targets much larger than 800 minutes in area. The Graham, Brown and Mote theory has been extended to targets as large as 3000 minutes squared.

Lamar's curves, Figure 8 for total flux are similar to the curves (Figs. 9, 10, 11) which we derived from Hardy's data.

The formula implies that as (R) perimeter increases the total flux must also increase, a conclusion that agrees with the data that has been collected; it also implies that as the area (A_1) of useful flux increases, the contrast requirements for detection decreases.

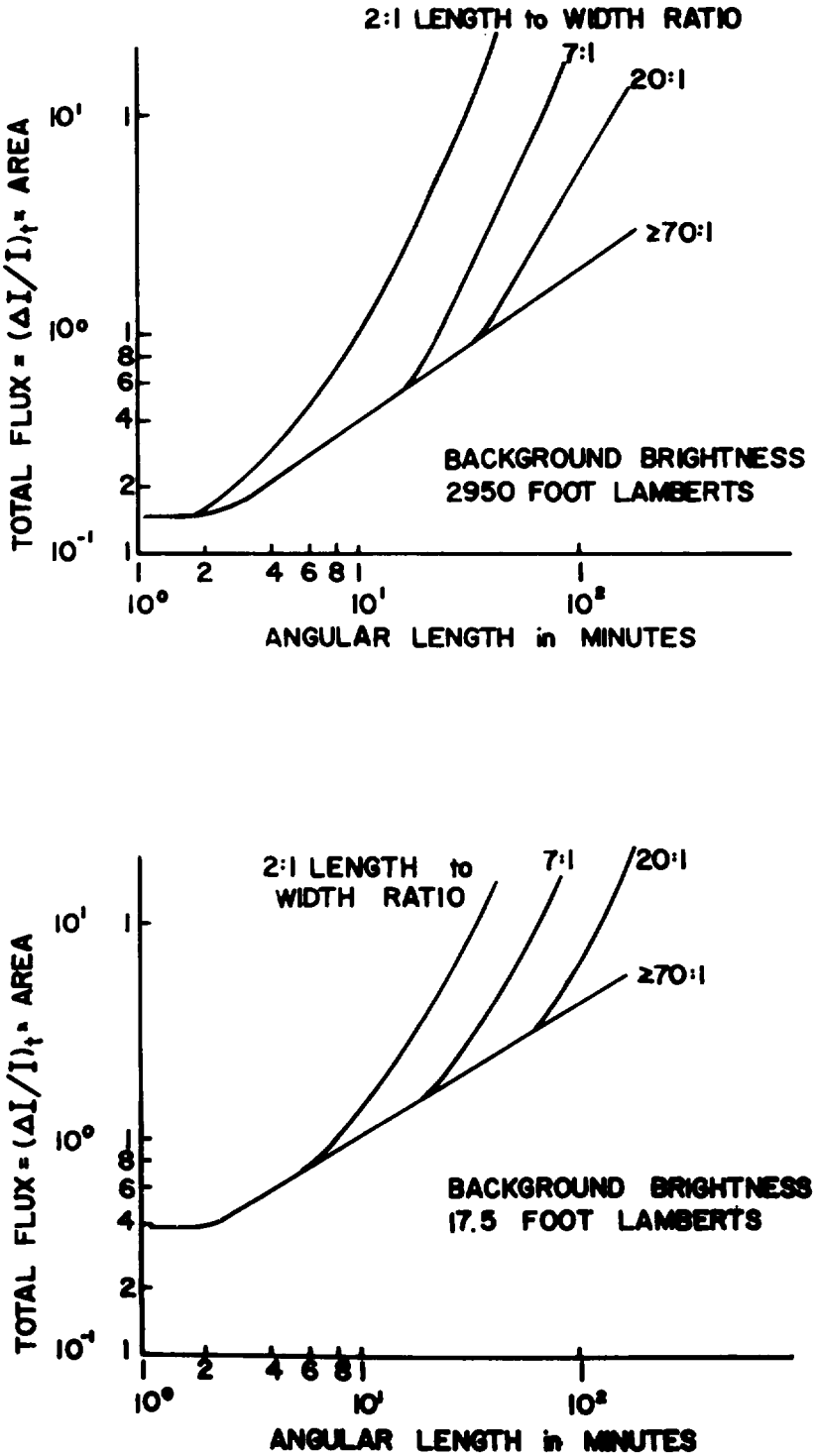

Fig. 8. RELATION BETWEEN TOTAL FLUX AND ANGULAR LENGTH OF TARGET-FOVEAL VISION FROM REFERENCE 9

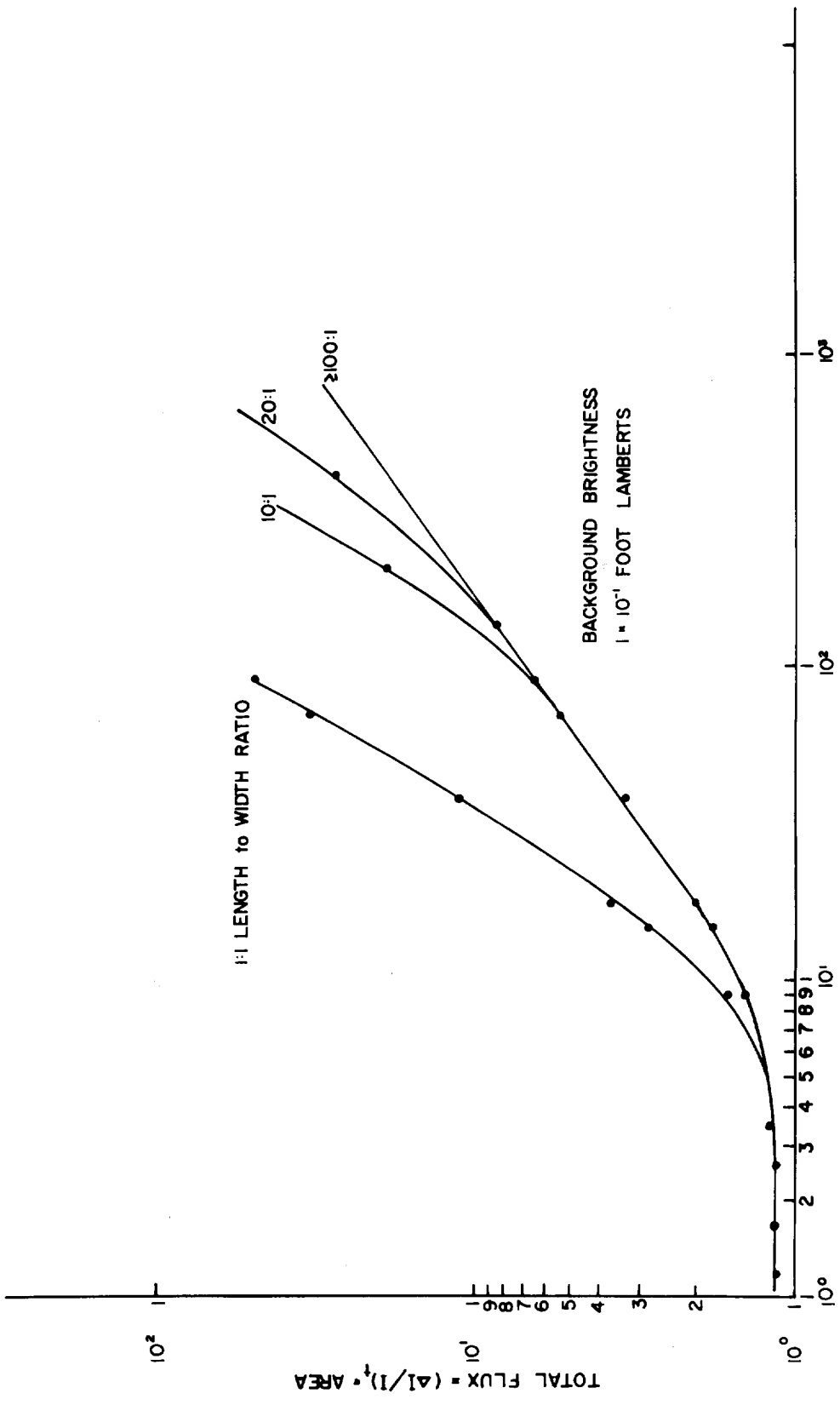

Fig. 9. RELATION BETWEEN TOTAL FLUX AND ANGULAR LENGTH OF TARGET
POINTS CALCULATED FROM REFERENCE 9 DATA AND PLOTTED BY INSPECTION

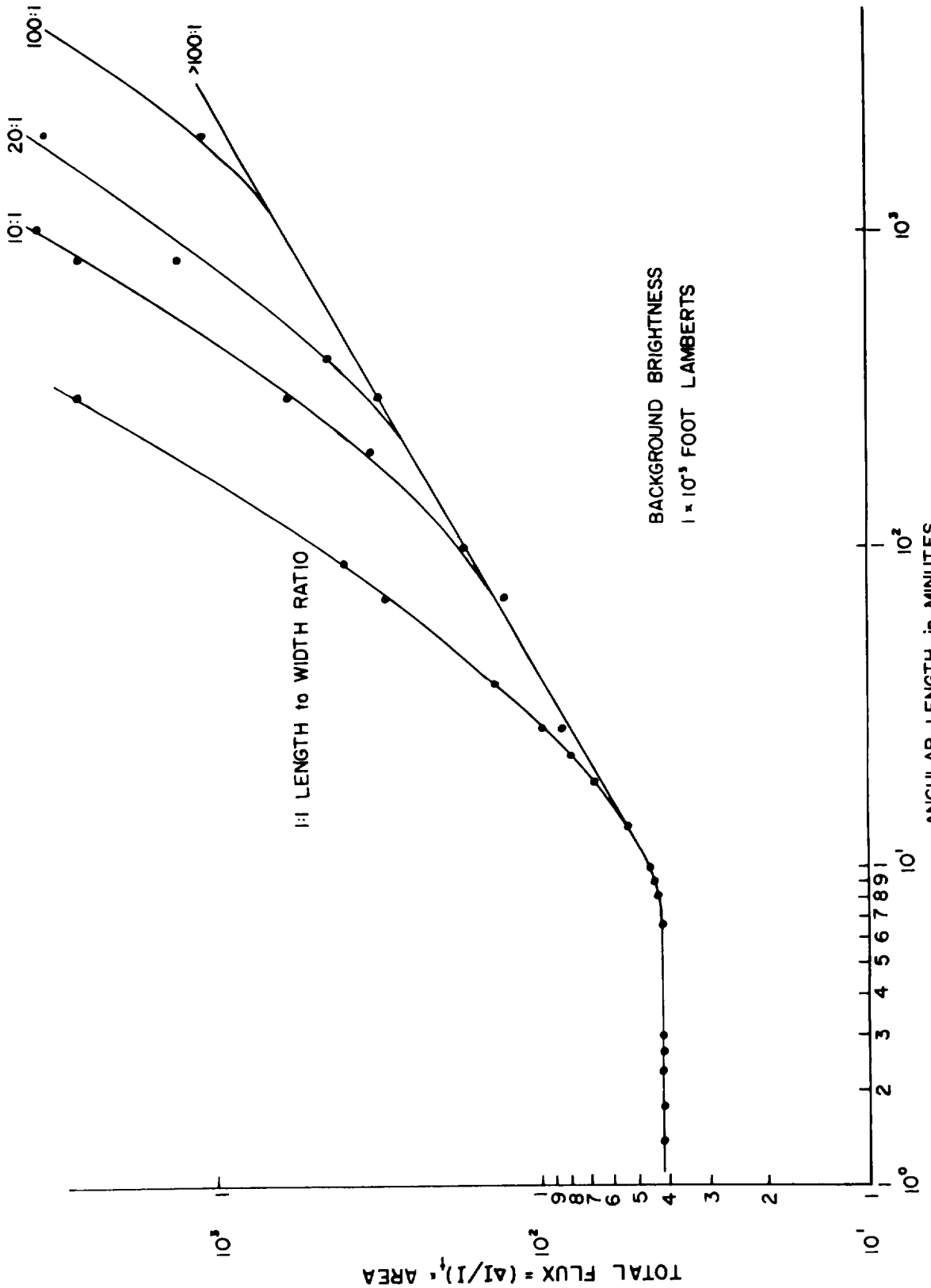

Fig. 10. RELATION BETWEEN TOTAL FLUX AND ANGULAR LENGTH OF TARGET POINTS CALCULATED FROM REFERENCE 9 DATA AND PLOTTED BY INSPECTION

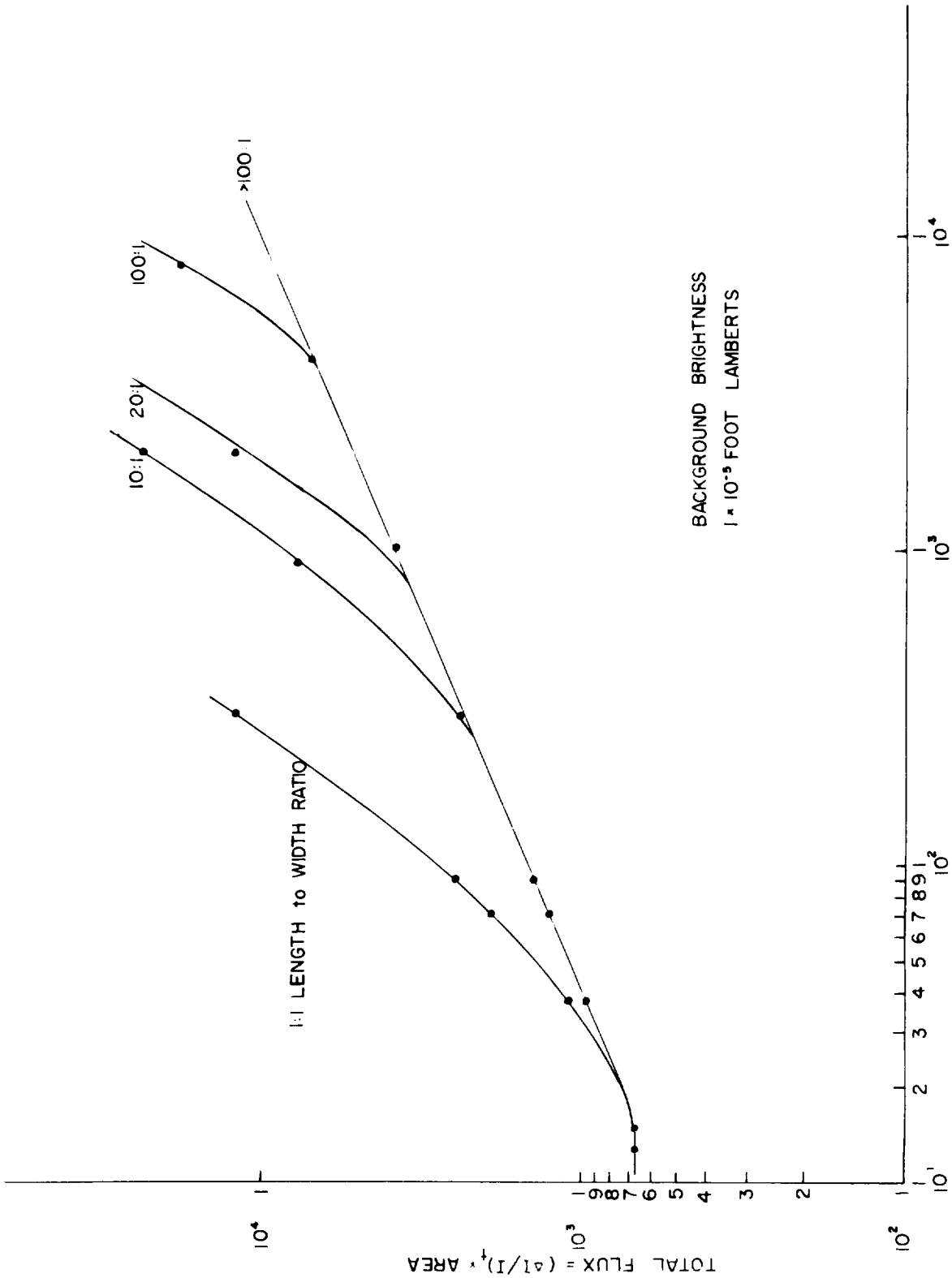

Fig. 11. RELATION BETWEEN TOTAL FLUX AND ANGULAR LENGTH OF TARGET
POINTS CALCULATED FROM REFERENCE 9 DATA AND PLOTTED BY INSPECTION

The formula for useful flux (F) is:

$$F = \left(\frac{\pi}{4} D_B^2\right) \cdot \left(\frac{\Delta I}{I}\right)_t - \frac{\pi}{4} \left(D_B - D_S\right)^2 \cdot \left(\frac{\Delta I}{I}\right)_t$$

where $D_B > D_S$

: D_B is the diameter of the target in minutes of arc.

D_S is the diameter of the smallest area of totally useful flux.

$$R = 2\pi\left(\frac{D}{2}\right) = \pi D$$

for circular targets with (R) perimeter.

Therefore: $$F = \frac{\pi}{4} D_S(2D_B - D_S) \cdot \left(\frac{\Delta I}{I}\right)_t$$

$$F = \left(\frac{\Delta I}{I}\right)_t \cdot A_1 \qquad (2)$$

Note that Equation 2 is merely a restatement of Equation 1 in which useful flux (F) has been substituted for CR^k.

$$F = \left(\frac{\Delta I}{I}\right)_t \cdot A_1 = CR^k \qquad (3)$$

We can solve for C by letting k = 0, the slope at the limit as angular length becomes very small. Then

$$F = CR^0 = C \qquad (4)$$

for targets where D_B is less than D_S. Since the curve approaches zero slope at the extreme left, the F value can be read from the ordinate. Note that the useful flux limit for very small target thresholds is larger for lower level backgrounds by virtue of the increased contrast requirements against very dark backgrounds.

For example, the curves for different length to width ratios against a 10^{-3} foot-lambert background repeatedly intercept the useful flux curve at 10-minute widths (Fig. 10). This appears to be a critical limit above which the flux emitted is no longer totally useful. The width of the band of useful flux for 10^{-3} foot-lambert background is therefore $D = \frac{10}{2} = 5$ (Fig. 12).

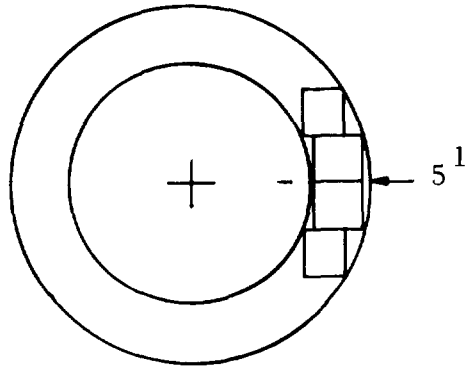

Fig. 12. TARGET ASSUMED TO BE CIRCULAR
(Shows the area of useful flux for the case of 10^{-3} Foot-Lamberts background.)

Useful flux $F = \left(\frac{\Delta I}{I}\right)_t \cdot A_1 = CR^k$. For background of 10^{-3} foot-lambert, slope $= k \simeq 0$ at $\simeq 10$ minutes which, from Equation 4, permits

$$F = C = 46.0$$

at the intercept of the 1:1 curve at approximately 10 minutes length. Solving for k, the slope above 10 minutes of arc,

$$\log \left[\left(\frac{\Delta I}{I}\right)_t \cdot \frac{A_1}{C}\right] \Big/ \log(R) = k$$

By substituting Hardy's data we know all of the terms except for (C) the constant and (k) the slope of the curve. The two unknowns can be solved for by picking two points on the curve and fitting the equation,

$$F = \left(\frac{\Delta I}{I}\right)_t A_1 = CR^k$$

to the data. Since the curve has a constant slope (k), the two points picked are shown on Table 3.

TABLE 3

Data Used to Calculate Constants k and C

Minutes of Arc (Subtend by Target)	Contrast Ratio	(R) Perimeter of Surface Square or Equivalent Circle	Useful Flux $\left(\frac{\Delta I}{I}\right)_t \cdot A_1$
25.84	.161	81.178752	52.724
80.75	.0607	253.6836	72.226

$$\left(\frac{\Delta I}{I}\right)_t \cdot A_1 = CR^k$$

$$(52.724) = C\,(81.178752)^{k} \qquad \text{(a)}$$

$$(72.226) = C\,(253.6836)^{k} \qquad \text{(b)}$$

$$\frac{(52.724)}{(81.178752)^{k}} = C$$

substitute the value of (C) that we get from (a) into Equation (b) we get

$$\frac{\log\,(1.36988)}{\log\,(3.12500)} = k$$

Therefore:

$$\begin{cases} .276210002 = k \\ 15.65313285 = C \end{cases}$$

Graphs were done for 10^{-1}, 10^{-3}, and 10^{-5} foot-lamberts, using the useful flux idea to predict level of threshold contrast for rectangular targets of 1:1, 10:1, 20:1 and 100:1 ratios (Figs. 13, 14, 15).

Comparison of Blackwell's curves (Fig. 2) for 10^{-5} foot-lamberts with Figure 15, which was derived from Hardy's data using Lamar's useful flux method, show the similar results for targets from 1.0 to 300.0 square minutes of arc. Hence, it appears that the useful flux method, which Lamar demonstrated for high brightness backgrounds, can also be applied to low brightness backgrounds involving scotopic vision. This provides a way of applying Blackwell's and Hardy's data to illuminated surfaces having extended or asymmetric shapes.

ATTENUATION AND SCATTER

Duntley (4) provided a mathematical model for apparent luminance of a light source at a given slant range through the atmosphere. He assumed that in passing through the atmosphere the transmitted radiant flux, t or s (Fig. 16) will be diminished by absorption and scattering, and these changes, $\left(\frac{dt}{dr}\right)$ and $\left(-\frac{ds}{dr}\right)$, for upward and downward, respectively, will be proportional to the flux β_r and q were called the constants of proportionality. τ_r and σ_r were scattering-rate

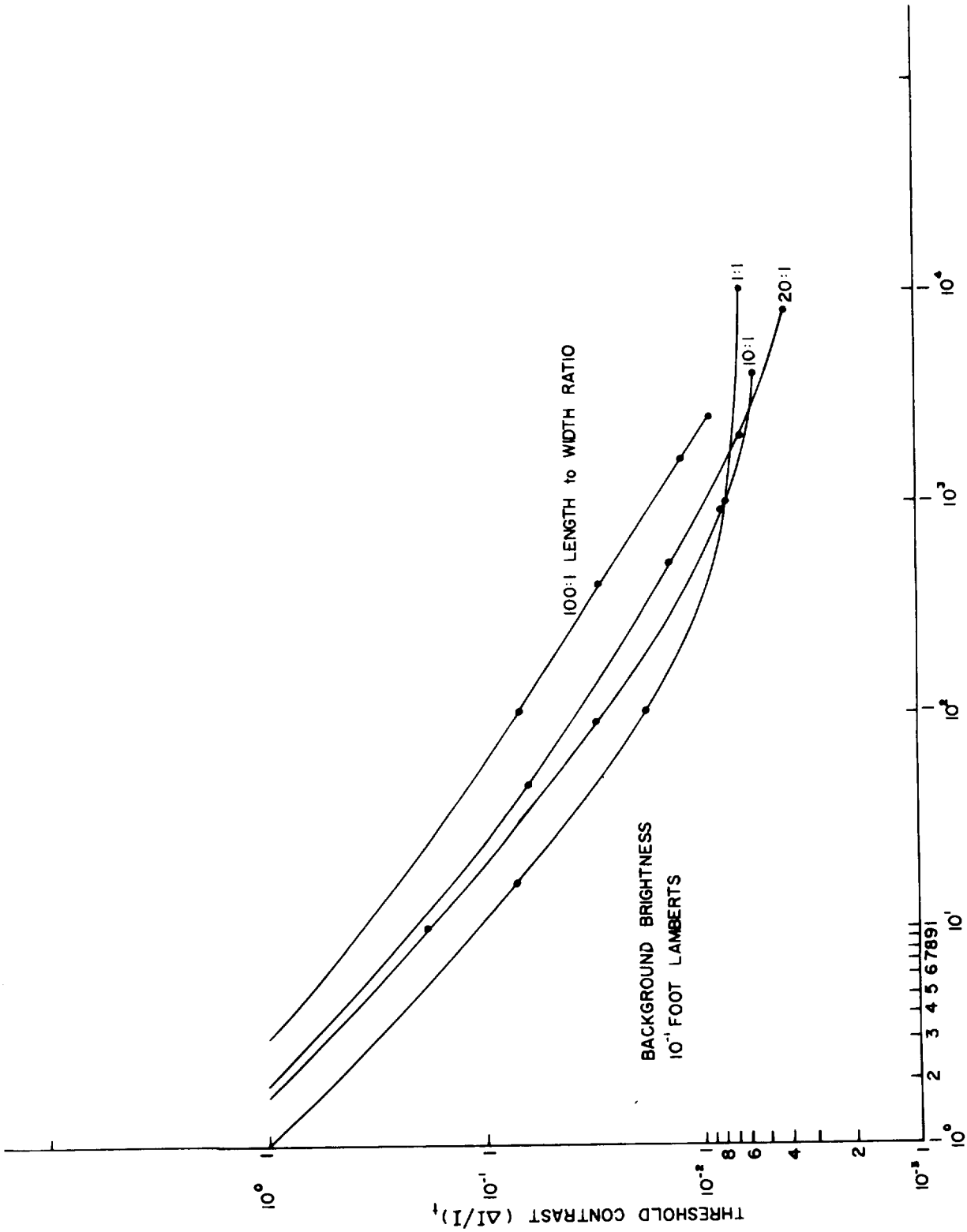

Fig. 13. RELATION BETWEEN THRESHOLD CONTRAST AND ANGULAR AREA FOR RECTANGULAR TARGETS WITH DIFFERENT LENGTH TO WIDTH RATIOS

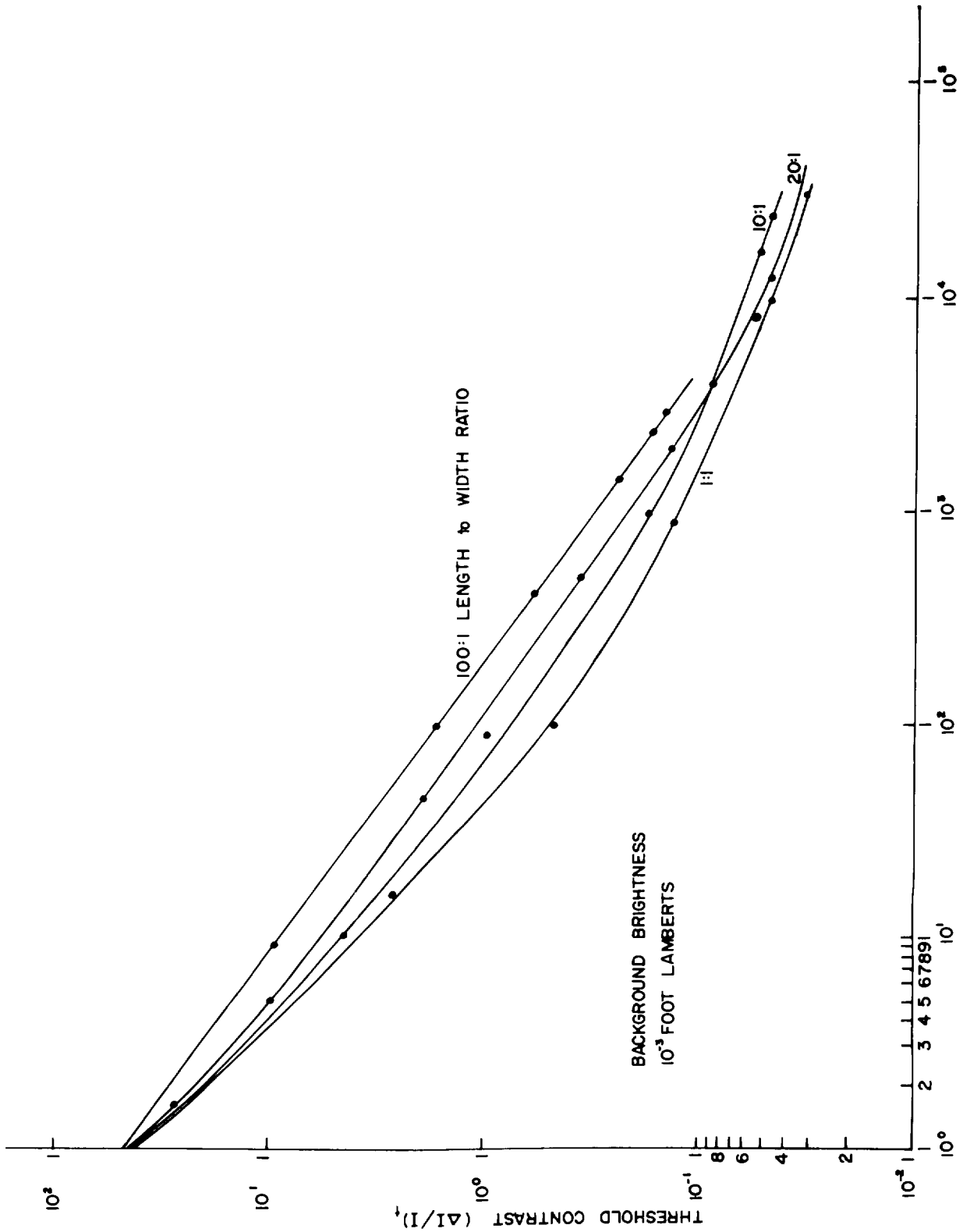

Fig. 14. RELATION BETWEEN THRESHOLD CONTRAST AND ANGULAR AREA FOR RECTANGULAR TARGETS WITH DIFFERENT LENGTH TO WIDTH RATIOS

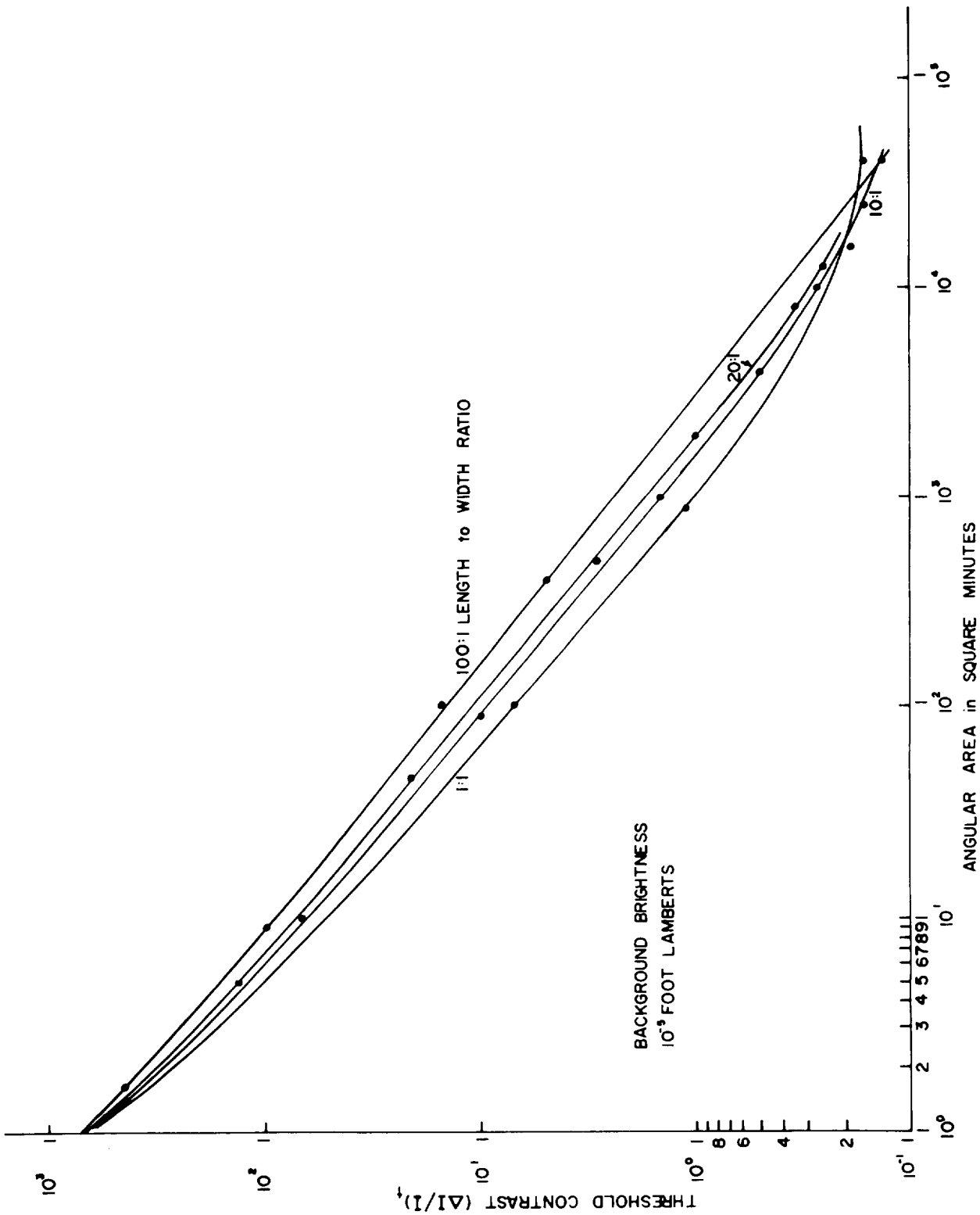

Fig. 15. RELATION BETWEEN THRESHOLD CONTRAST AND ANGULAR AREA FOR RECTANGULAR TARGETS WITH DIFFERENT LENGTH TO WIDTH RATIOS

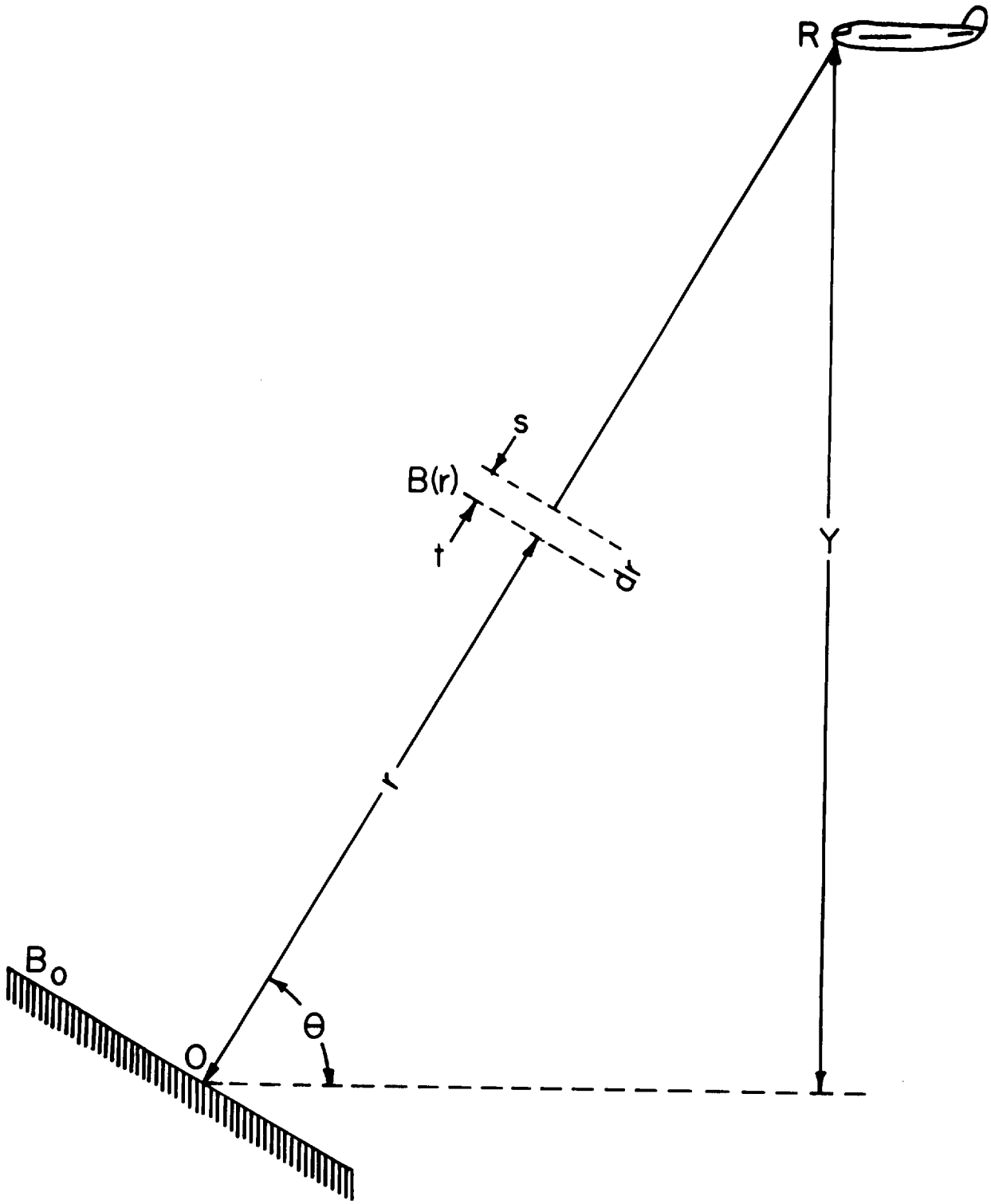

Fig. 16. ILLUSTRATING THE TWO CONSTANT THEORY

coefficients. β_r was the atmospheric attenuation coefficient, and q was the spectral radiant density of space light, which is the same at all points. The differential equations that relate all of these elements are:

$$\frac{dt}{dr} = -\beta_r t + \tau_r q \qquad (5)\ \text{(observer looking downward)}$$

$$-\frac{ds}{dr} = -\beta_r s + \sigma_r q \qquad (6)\ \text{(observer looking upward)}$$

By replacing $\beta_r = \beta_o f(r)$

$\tau_r = \tau_o f(r)$ and

$\sigma_r = \sigma_o f(r)$, where β_o, τ_o, and σ_o are the values assumed at the lower end of the path of sight, Equations 5 and 6 become:

$$\int_{W_o}^{W_R} \frac{dt}{-\beta_o t + \tau_o q} = \int_{O}^{R} f(r)dr \qquad (7)\ \text{(observer looking downward)}$$

$$\int_{W_R}^{W_o} \frac{ds}{-\beta_o s + \tau_o q} = -\int_{R}^{O} f(r)dr \qquad (8)\ \text{(observer looking upward)}$$

where W_R and W_o are values of light flux as defined at R and O respectively.

In the case of a horizontal path of sight through a homogeneous atmosphere, $f(r) = 1$ since β_o, τ_o, and σ_o are the same at all points. In the case of an inclined path of sight, $f(r) \neq 1$, because the air density and particles in suspension decrease with increasing altitude. Let $\bar{R}$ be the optical slant range. Then

$$\bar{R} = \int_o^R f(r)dr \tag{9}$$

Performing the integration indicated in (7):

$$\bar{R} = \int_o^R f(r)dr = \int_{W_o}^{W_R} \frac{dt}{-\beta_o t + \tau_o q} = -\frac{1}{\beta_o} \log_e(-\beta_o t + \tau_o q) \Big|_{W_o}^{W_R}$$

$$\bar{R} = -\frac{1}{\beta_o} \log_e(-\beta_o W_R + \tau_o q) + \frac{1}{\beta_o} \log_e(-\beta_o W_o + \tau_o q)$$

$$\bar{R} = \frac{1}{\beta_o} \left[\log_e(-\beta_o W_o + \tau_o q) - \log_e(-\beta_o W_R + \tau_o q)\right]$$

$$\beta_o \bar{R} = [\log_e(-\beta_o W_o + \tau_o q) - \log_e(-\beta_o W_R + \tau_o q)]$$

$$e^{\beta_o \bar{R}} = (-\beta_o W_o + \tau_o q) \Big/ (-\beta_o W_R + \tau_o q)$$

$$e^{\beta_o \bar{R}} (-\beta_o W_R + \tau_o q) = (-\beta_o W_o + \tau_o q)$$

$$-\beta_o W_R e^{\beta_o \bar{R}} = -e^{\beta_o \bar{R}} \tau_o q - \beta_o W_o + \tau_o q$$

$$W_R = \frac{-e^{\beta_o \bar{R}} \tau_o q - \beta_o W_o + \tau_o q}{-\beta_o e^{\beta_o \bar{R}}}$$

$$W_R = \frac{\tau_o q}{\beta_o} (1 - e^{-\beta_o \bar{R}}) + W_o e^{-\beta_o \bar{R}} \qquad (10)$$

In a similar manner performing the integration indicated in Equation (8), we get:

$$W_R = \frac{\tau_o q}{\beta_o} (1 - e^{-\beta_o \bar{R}}) + W_o e^{-\beta_o \bar{R}} \qquad (11)$$

where W_R and W_o are the flux as defined at R and 0 respectively.

Substituting B_o, inherent luminance, and B_R, apparent luminance, for W_o and W_R, respectively, in Equations (10) and (11):

$$B_R = \frac{\tau_o q}{\beta_o} (1 - e^{-\beta_o \bar{R}}) + B_o e^{-\beta_o \bar{R}} \qquad (12)$$

$$B_R = \frac{\tau_o q}{\beta_o} (1 - e^{-\beta_o \bar{R}}) + B_o e^{-\beta_o \bar{R}} \qquad (13)$$

Visibility

Luminance differences are exponentially attenuated.

$$(B_{R1} - B_{R2}) = (B_{01} - B_{02}) e^{-\beta_o \bar{R}} \qquad (14)$$

where B_{R1} and B_{01} refer to the apparent and inherent luminances of the object; and B_{R2} and B_{02} refer to the luminances of the background. Equation (14) above is for the horizontal case. Since target visibility is best described in terms of contrast thresholds, the Equations (12), (13) and (14) will be used to determine contrast

ratios. The contrast ratio is the ratio between the brightness of the object minus the brightness of the background divided by the brightness of the background (assuming the object is the brighter). Let

C_0 = inherent contrast

C_R = apparent contrast

Then, the contrasts are defined as:

$$C_0 = \frac{B_{01} - B_{02}}{B_{02}} \tag{15}$$

$$C_R = \frac{B_{R1} - B_{R2}}{B_{R2}} \tag{16}$$

Equation (14) when divided through by $B_{02} \cdot B_{R2}$ becomes

$$C_R = \frac{B_{02}}{B_{R2}} \; C_0 e^{-\beta_o \bar{R}} \tag{17}$$

The apparent luminance of the sky as seen from the ground in the vicinity of the target is:

$$B_{R2} = \frac{\tau_o q}{\beta_o} \left(1 - e^{-\beta_o \bar{R}_{o,\infty}}\right) \tag{18}$$

The inherent luminance of the sky (as viewed from the region of the target) is

$$B_{02} = \frac{\tau_o q}{\beta_o} \left(1 - e^{-\beta_o \bar{R}_{R,\infty}}\right) \tag{19}$$

which can be derived from Equation (13).

Since $B_o e^{-\beta_o \bar{R}} \longrightarrow 0$ as $\bar{R} \longrightarrow \infty$

Visibility Upward

Substituting Equations (18) and (19) into $C_R = \frac{B_{02}}{B_{R2}} C_o e^{-\beta_o \bar{R}}$ yields the case of atmospheric reduction in contrast for an observer looking upward along an inclined path.

$$C_R = C_o e^{-\beta_o \bar{R}} \left[\frac{1 - e^{-\beta_o \bar{R}_{R,\infty}}}{1 - e^{-\beta_o \bar{R}_{o,\infty}}} \right] \qquad (20)$$

Downward Visibility

$$B_R = \frac{\tau_o q}{\beta_o} (1 - e^{-\beta_o \bar{R}}) + B_o e^{-\beta_o \bar{R}}$$

From observer to ground:

$$B_{R2} = \frac{\tau_o q}{\beta_o} (1 - e^{-\beta_o \bar{R}_{o,G}}) + B_o e^{-\beta_o \bar{R}_{o,G}}$$

From target to ground (assuming target on ground):

$$B_{02} = \frac{\tau_o q}{\beta_o} (1 - e^{-\beta_o R_{o,o}}) + B_o e^{-\beta_o R_{o,o}}$$

since $\bar{R}_{o,o} = 0$

$$B_{02} = B_o$$

substituting into Equation (17):

$$C_R = C_o \left[\frac{B_{02} e^{-\beta_o \bar{R}}}{\frac{\tau_o q}{\beta_o}(1 - e^{-\beta_o \bar{R}_{o,G}}) + B_{02} e^{-\beta_o \bar{R}_{o,G}}} \right]$$

$$C_R = C_o \left[\frac{B_{02} e^{-\beta_o \bar{R}}}{\frac{\tau_o q}{\beta_o} - \frac{\tau_o q e^{-\beta_o \bar{R}_{o,G}}}{\beta_o} + \frac{\beta_o B_{02} e^{-\beta_o \bar{R}_{o,G}}}{\beta_o}} \right]$$

$$C_R = C_o \left[\frac{B_{02} \beta_o e^{-\beta_o \bar{R}}}{\tau_o q - \tau_o q e^{-\beta_o \bar{R}_{o,G}} + \beta_o B_{02} e^{-\beta_o \bar{R}_{o,G}}} \right]$$

$$C_R = C_o \left[\frac{1}{\frac{\tau_o q - \tau_o q e^{-\beta_o \bar{R}_{o,G}} + \beta_o B_{02} e^{-\beta_o \bar{R}_{0,G}}}{\beta_o B_{02} e^{-\beta_o R_{o,G}}}} \right]$$

$$C_R = C_o \left[1 - \frac{\tau_o q}{\beta_o B_{02}} (1 - e^{\beta_o \bar{R}_{o,G}}) \right]^{-1} \qquad (21)$$

Where $\frac{B_m}{B_o} = \frac{\tau_o q}{\beta_o B_{02}}$ (sky-ground ratio)

therefore Equation (21) becomes:

$$C_R = C_o \left[1 - \frac{B_m}{B_{o2}} (1 - e^{\beta_o \bar{R}_{o,G}}) \right]^{-1} \qquad (22)$$

TABLE 4

Sky-Ground Ratio

Sky Condition	Ground Condition	Sky-Ground Ratio
Overcast	Fresh snow	1
Overcast	Desert	7
Overcast	Forest	25
Clear	Fresh snow	0.2
Clear	Desert	1.4
Clear	Forest	5

For the general case of downward visibility for a target not on the ground:

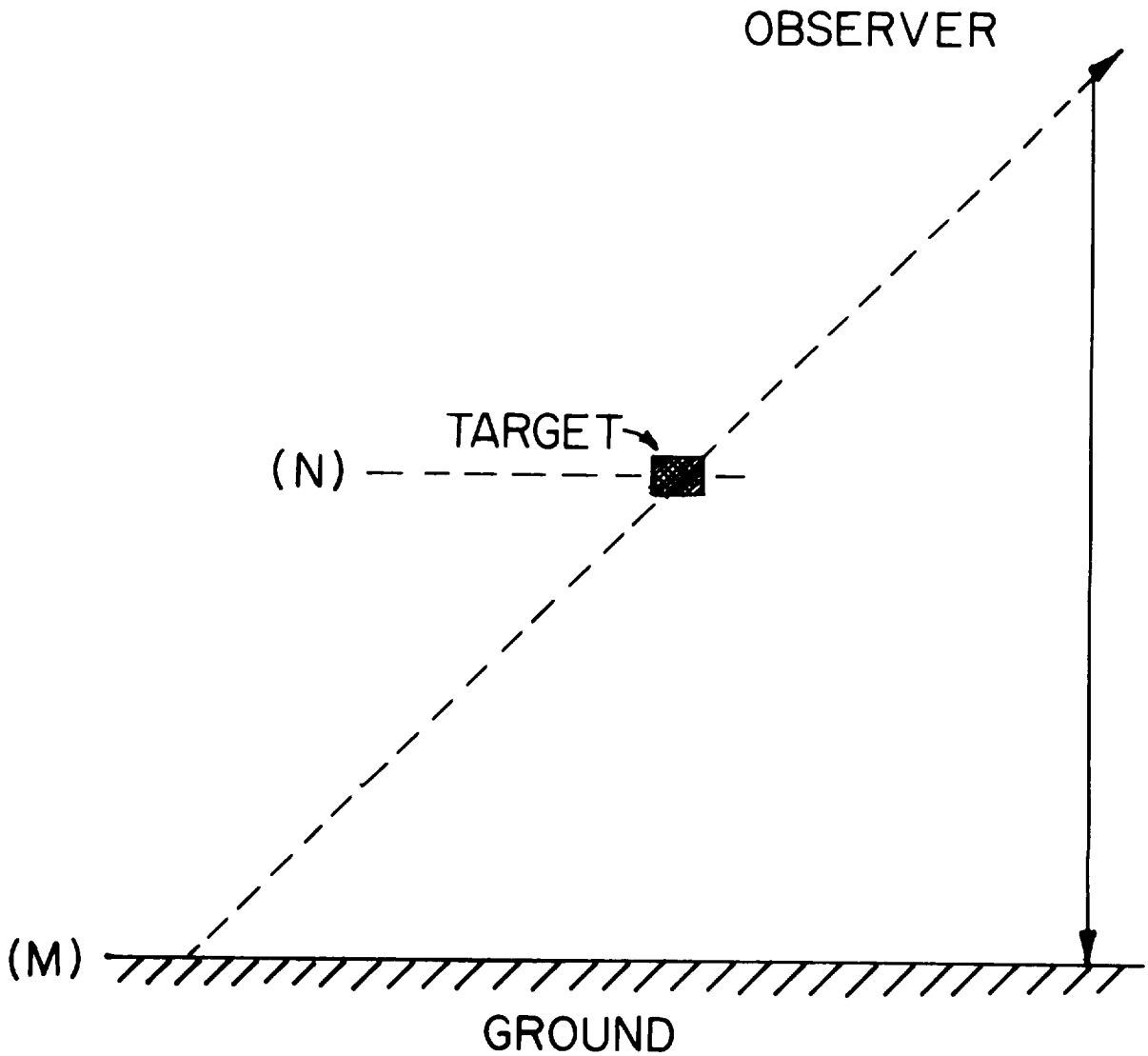

Fig. 17. FOR THE GENERAL CASE OF DOWNWARD VISIBILITY FOR A TARGET NOT ON THE GROUND

$$B_R = \frac{\tau_o q}{\beta_o} (1 - e^{-\beta_o \bar{R}}) + B_o e^{-\beta_o \bar{R}}$$

Observer to ground:

$$B_R = \frac{\tau_o q}{\beta_o} (1 - e^{-\beta_o \bar{R}_{o,M}}) + B_o e^{-\beta_o \bar{R}_{o,M}}$$

Target to ground:

$$B_o = \frac{\tau_o q}{\beta_o} (1 - e^{-\beta_o \bar{R}_{N,M}}) + B_o e^{-\beta_o R_{N,M}}$$

$$C_R = \frac{B_o}{B_R} C_o e^{-\beta_o \bar{R}_{o,N}}$$

$$C_R = C_o \left[\frac{\frac{\tau_o q}{\beta_o} (1 - e^{-\beta_o \bar{R}_{N,M}}) + B_o e^{-\beta_o \bar{R}_{N,M}}}{\frac{\tau_o q}{\beta_o} (1 - e^{-\beta_o \bar{R}_{o,M}}) + B_o e^{-\beta_o \bar{R}_{o,M}}} \right] e^{-\beta_o \bar{R}_{o,M}}$$

Since $B_M = \frac{\tau_o q}{\beta_o}$; $\frac{B_M}{B_o}$ = (sky-ground ratio)

$$C_R = C_o \left[\frac{\frac{B_M}{B_o} (1 - e^{-\beta_o \bar{R}_{N,M}}) + e^{-\beta_o \bar{R}_{N,M}}}{\frac{B_M}{B_o} (1 - e^{-\beta_o \bar{R}_{o,M}}) + e^{-\beta_o \bar{R}_{o,M}}} \right] e^{-\beta_o \bar{R}_{o,N}} \quad (23)$$

Equation (23) is for the general case of downward visibility (Fig. 17), target not on the ground.

The two cases above, Equations (20) and (23) together, are more precise versions of Duntley's law of contrast attenuation. These equations were derived for the computer programs used in this study.

Horizontal Visibility

$$C_R = C_o e^{-\beta_o \bar{R}_{o,R}} \tag{24}$$

Optical Slant Range ($\bar{R}$)

The optical slant range, $\bar{R}$, must be evaluated if the Equations (20), (23), and (24) are to be used correctly. Duntley suggested a method for determining $\bar{R}$. The method applied the equation of state of a perfect gas to the "standard atmosphere." The density of air is a function of the pressure, P, where M is the molecular weight, T is the absolute temperature, R is a physical constant known as the universal gas constant (8.314×10^7 ergs per mole-degree) and g is the gravitational constant. The fundamental equation allows the calculation of pressure throughout the atmosphere if the temperature and the molecular weight are known.

$$\frac{\Delta P}{P} = -\frac{Mg}{RT} \Delta h$$

where h is altitude above sea level expressed in feet. Pressure at the altitudes of interest can be calculated by integrating the fundamental equation.

$$\int \frac{\Delta P}{P} = -\int \frac{Mg}{RT} \Delta h$$

$$\log_e P = -\frac{Mg}{RT} h \quad \text{if} \quad \frac{Mg}{RT} = k \text{ constant}$$

Therefore,

$$P = e^{-kh} \tag{25}$$

which describes the standard atmosphere. The optical standard atmosphere is represented by Table 5, which gives the relative molecules per unit volume for each altitude.

TABLE 5

Relative Density of Air Due to Altitude

Altitude in Feet	Relative Number of Molecules Per Unit Volume
0	1.000
1.000	0.956
2.000	0.918
3.000	0.878
4.000	0.841
5.000	0.804
6.000	0.770
7.000	0.736
8.000	0.703
9.000	0.672
10.000	0.642
12.000	0.586
14.000	0.534
16.000	0.485
18.000	0.440
20.000	0.399
22.000	0.361
24.000	0.326
26.000	0.295
28.000	0.266
30.000	0.239

This relationship is described by an equation of the form (25). Using the data from Table 5, the following equation is derived:

$$\frac{N}{N_o} = e^{-h/21,700} \qquad (26)$$

where N_0 is the number of molecules per unit volume at sea level, N is the number of molecules at altitude h.

Along any slant path $h = r \sin \theta$. Thus if $f(r) = (N/N_0)$.. a generalized form of Equation (9) becomes:

$$\bar{R} = \int_{R_1}^{R_2} f(r)\,dr = \int_{R_1}^{R_2} e^{-r \sin\theta/21,700}\, dr$$

integrating we get:

$$\bar{R} = \int_{R_1}^{R_2} e^{-\frac{\sin\theta}{21,700} r}\, dr$$

$$\bar{R} = \frac{1}{-\frac{\sin\theta}{21,700}} e^{-\frac{\sin\theta}{21,700} r} \Bigg|_{R_1}^{R_2}$$

$$\bar{R} = -21,700 \csc\theta \left[e^{-R_2 \sin\theta/21,700} - e^{-R_1 \sin\theta/21,700}\right]$$

$$\bar{R} = 21,700 \csc\theta \left[e^{-R_1 \sin\theta/21,700} - e^{-R_2 \sin\theta/21,700}\right] \quad (27)$$

where $R_2 > R_1$

In the special case of the observer at sea level looking upward

$$\bar{R} = 21,700 \csc\theta \left[1 - e^{-R_2 \sin\theta/21,700}\right]$$

For non-standard conditions the description of the atmosphere can be accomplished by partitioning the volume into levels of density and attenuation.

Graphs to follow describe the brightnesses required of 20 square inch surface lamps such as electroluminance panels (EL) for a number of ground-sky ratios and attenuation levels, with background brightnesses of 10^{-3}, 10^{-4}, and 10^{-5} foot-lamberts (Figs. 18, 19, 20, 21, 22, 23, 24, 25 and 26).

These curves describe 0.50 probability of detection thresholds using Lamar's idea of useful flux and the law of attenuation and scatter from Duntley. The curves show the relationship between foot-lamberts brightness required on the EL panel and slant ranges, with sky-ground ratios of 5.0 and 25.0 for clear forest and over cast forest, respectively. Slant angle is 30^{o} with respect to the ground. The transmissivity level is given in per mile (5280 ft.).

TIME AS A FACTOR OF INCREASING THE PROBABILITY OF DETECTION

The number of "looks" at a target which is in the visible range is important in determining detection of light sources. We know (a) that a given light becomes visible at a fixed distance; (b) how long the target will be in the visible range; and (c) how its relative velocity in minutes per second limits the number of "looks." If the target is not detected on the first look, how long will it take to look again; and if another "look" is taken, will the target be detected? These questions must be answered if we are to make a realistic prediction about the probability of detecting a light source. Change in position of the target implies that the distance will vary, hence the probability of detection will increase or decrease with each change in location.

The first step is to determine the time duration of target visibility.

To simplify the calculation of the interval during which the target will be detectable, where threshold contrast levels are met from point $P_1(x, y, z)$ to $P_2(-x, y, z)$, it is assumed that the target is moving in a straight path at constant velocity and constant altitude (Fig. 27). Once we know the duration of time that the target will be detectable, we must estimate how often a person will look. Hence, how long is a "look" or, more precisely, a search cycle of the field?

Graham and Kemp (5) analyzed brightness discrimination as influenced by the duration of ΔI. For any given background brightness the product of threshold contrast and exposure time $\left[\left(\Delta I/I\right)_t \cdot t\right]$ was constant below a critical

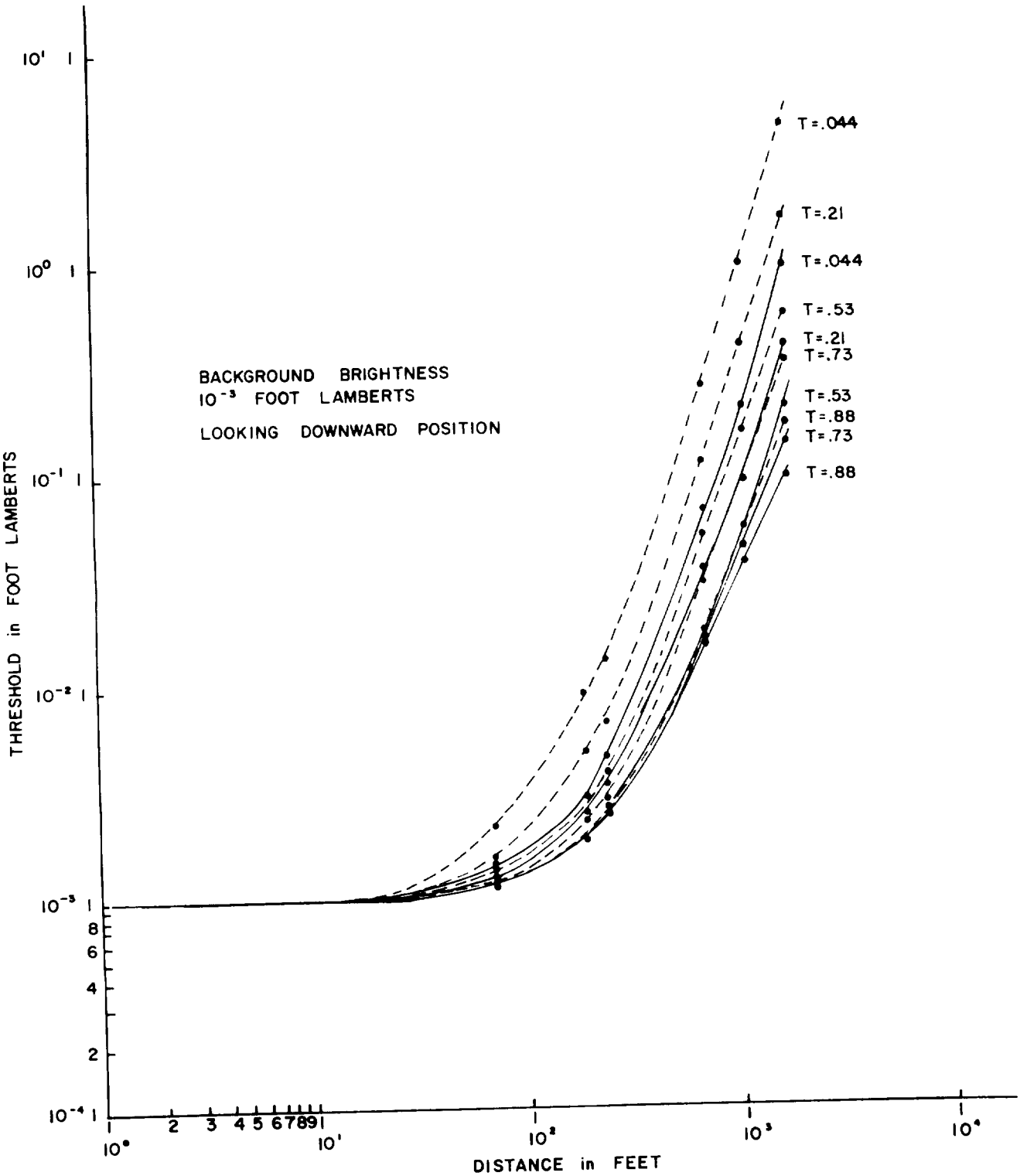

Fig. 18. RELATION BETWEEN THRESHOLD REQUIREMENTS FOR EL-PANEL (SLANT RANGE) AND DISTANCE

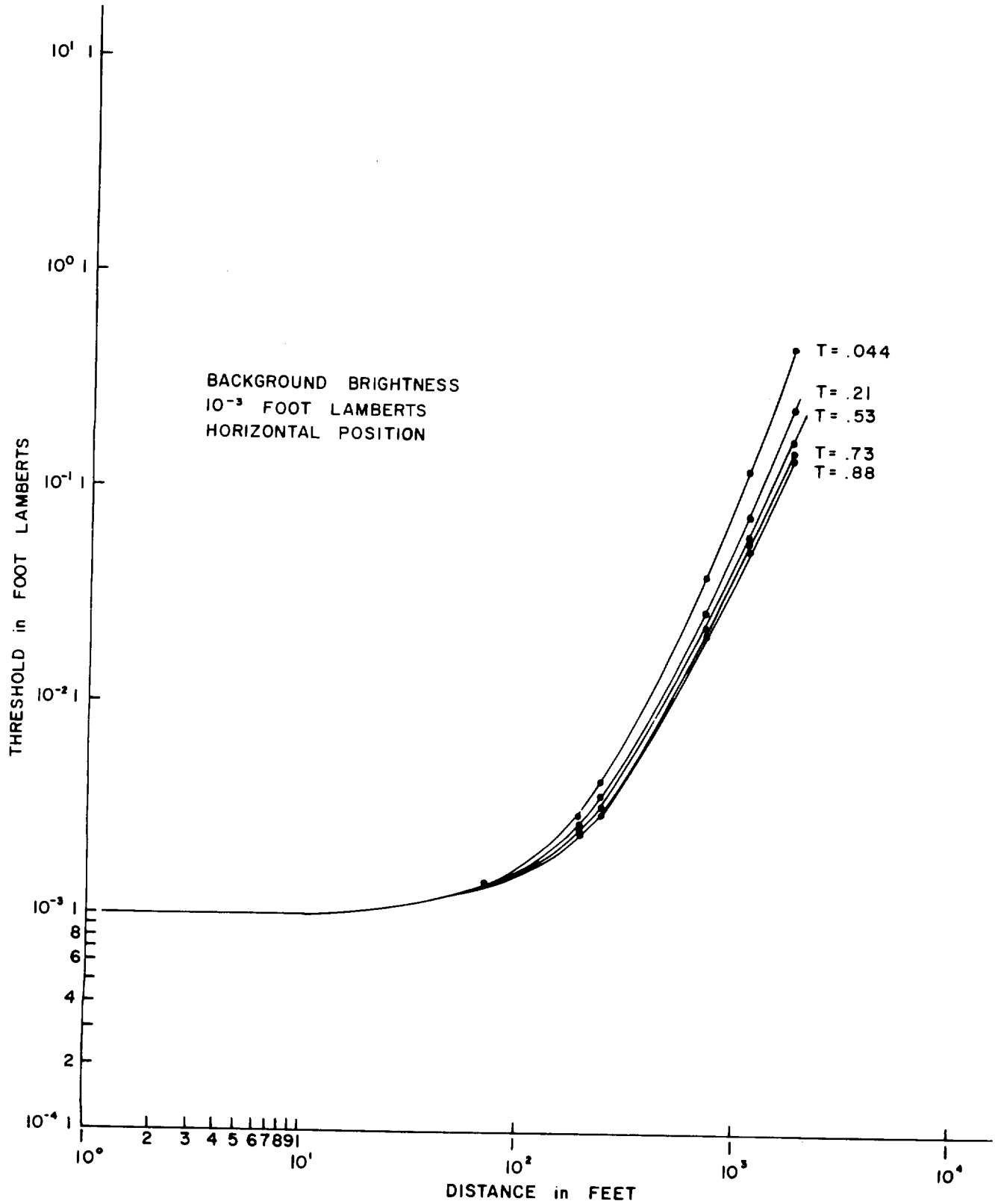

Fig. 19. RELATION BETWEEN THRESHOLD REQUIREMENTS FOR EL-PANEL (SLANT RANGE) AND DISTANCE

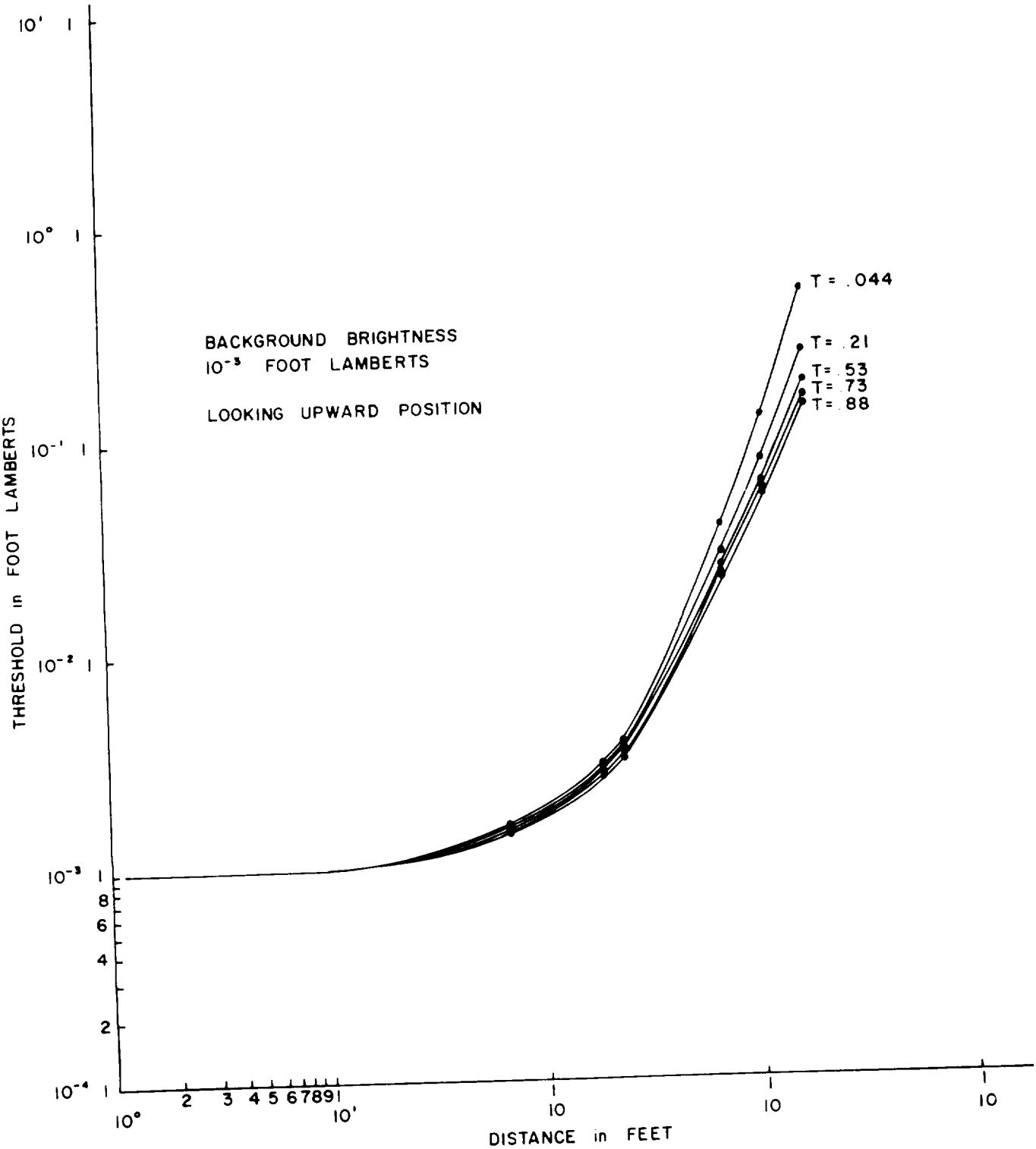

Fig. 20. RELATION BETWEEN THRESHOLD REQUIREMENTS FOR EL-PANEL (SLANT RANGE) AND DISTANCE

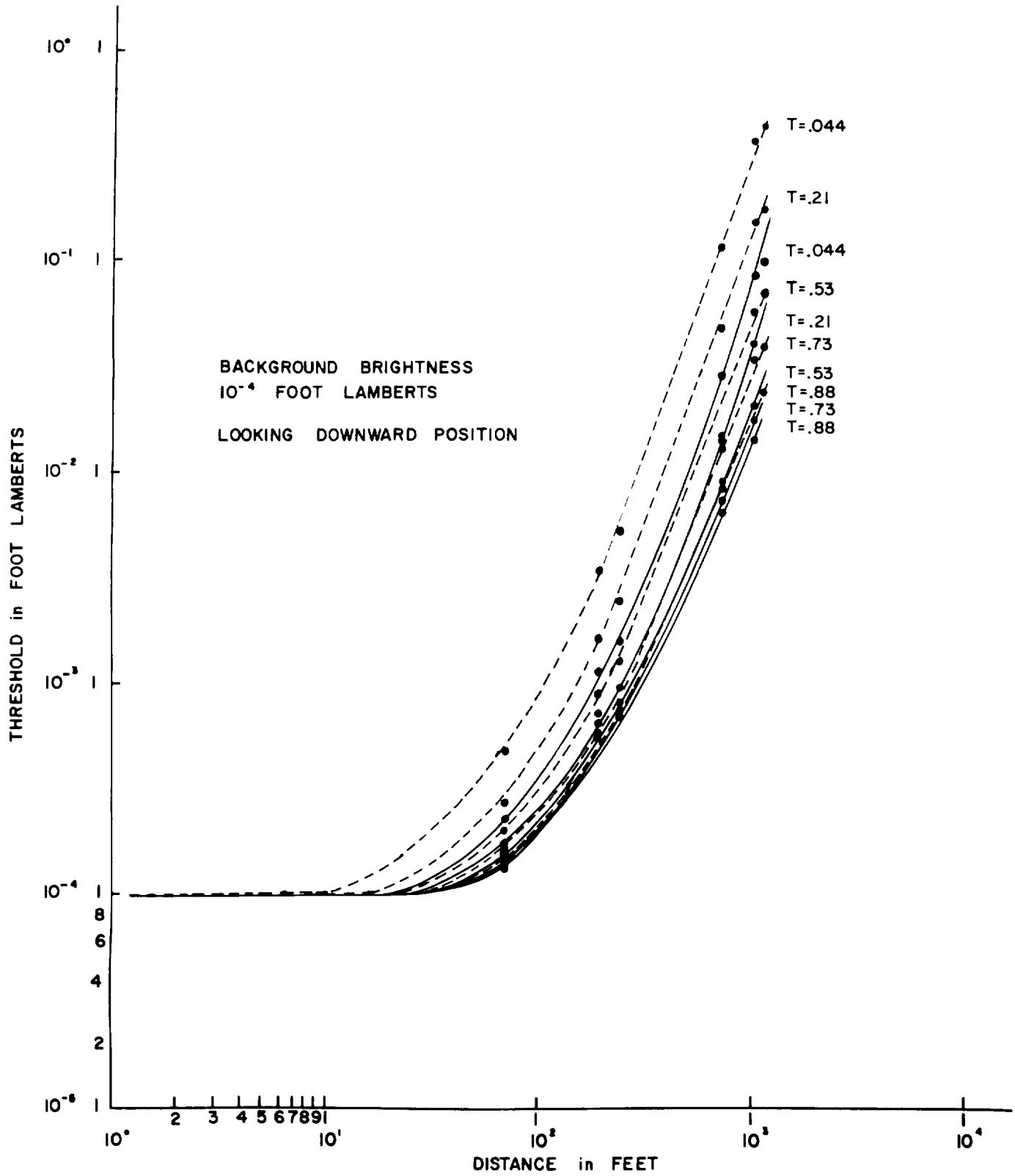

Fig. 21. RELATION BETWEEN THRESHOLD REQUIREMENTS FOR EL-PANEL (SLANT RANGE) AND DISTANCE

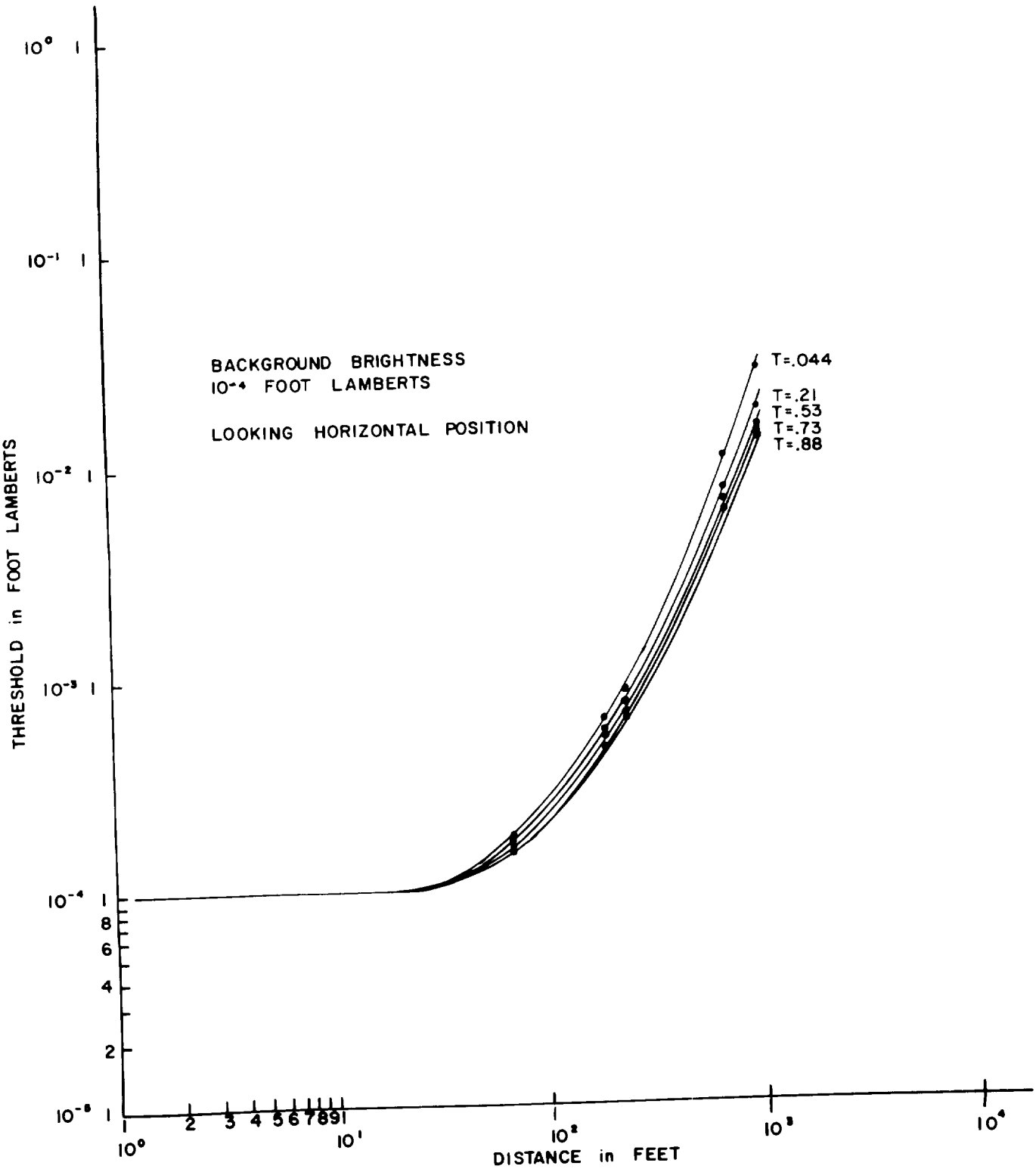

Fig. 22. RELATION BETWEEN THRESHOLD REQUIREMENTS FOR EL PANEL (SLANT RANGE) AND DISTANCE

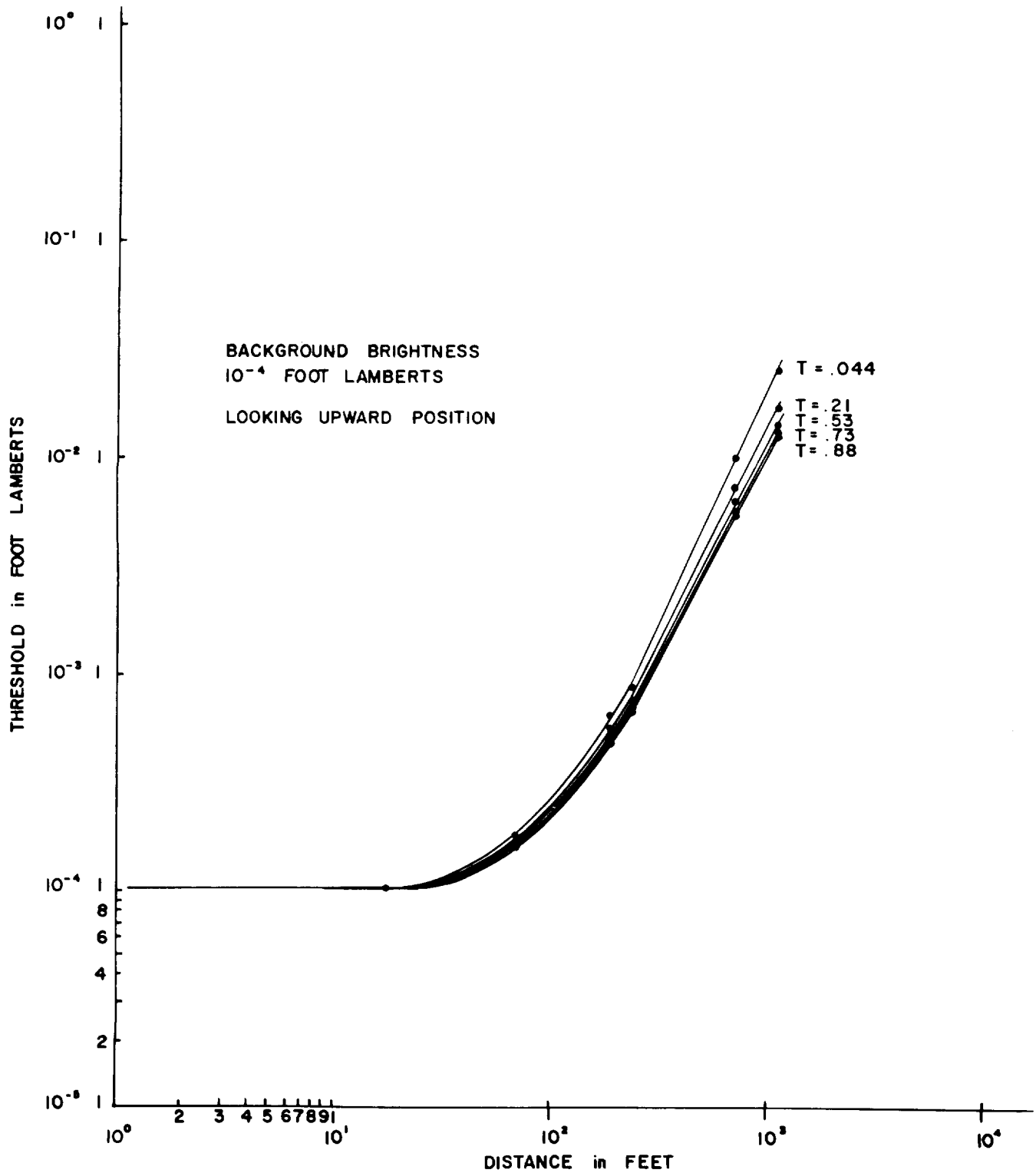

Fig. 23. RELATION BETWEEN THRESHOLD REQUIREMENTS FOR EL-PANEL (SLANT RANGE) AND DISTANCE

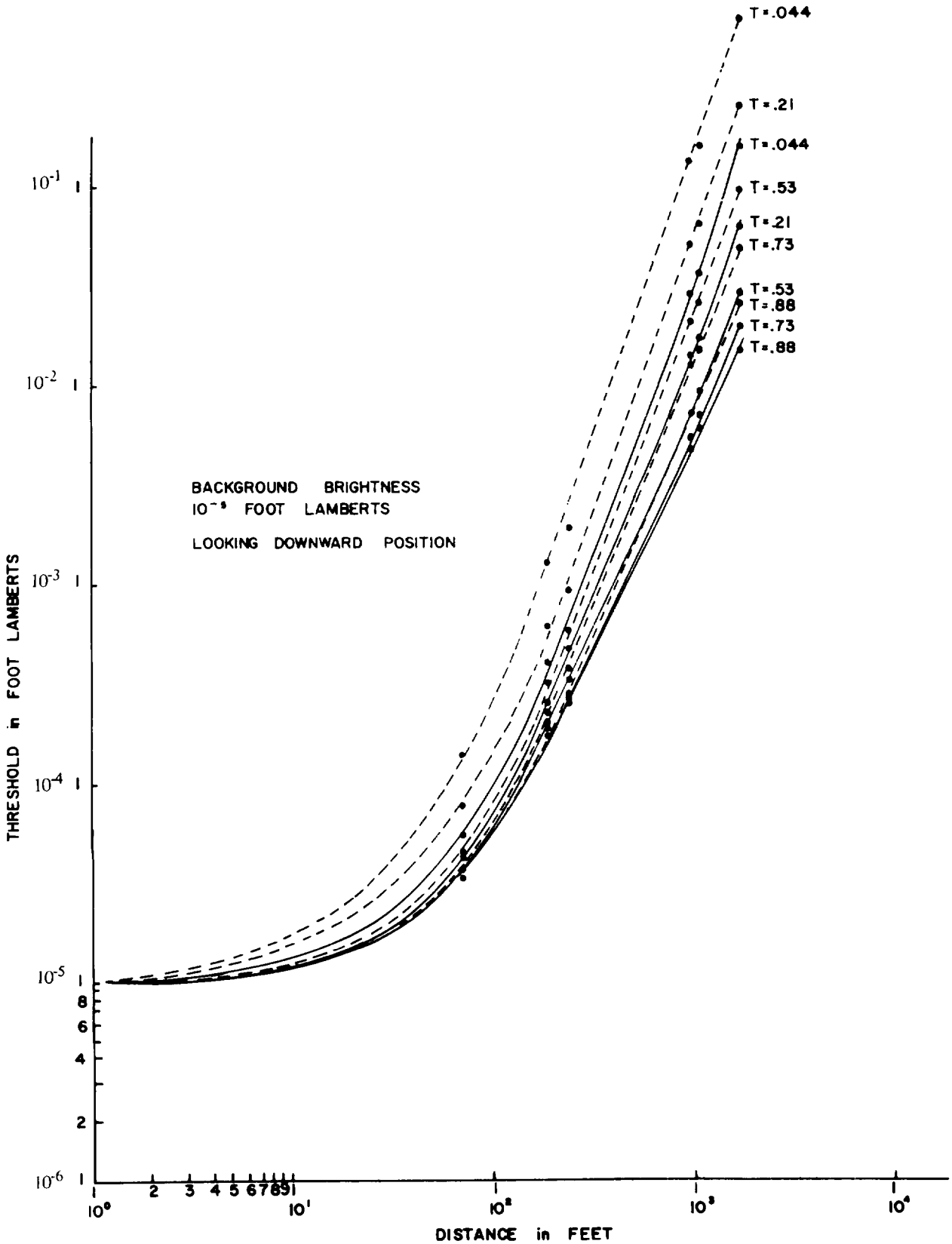

Fig. 24. RELATION BETWEEN THRESHOLD REQUIREMENTS FOR EL-PANEL (SLANT RANGE) AND DISTANCE

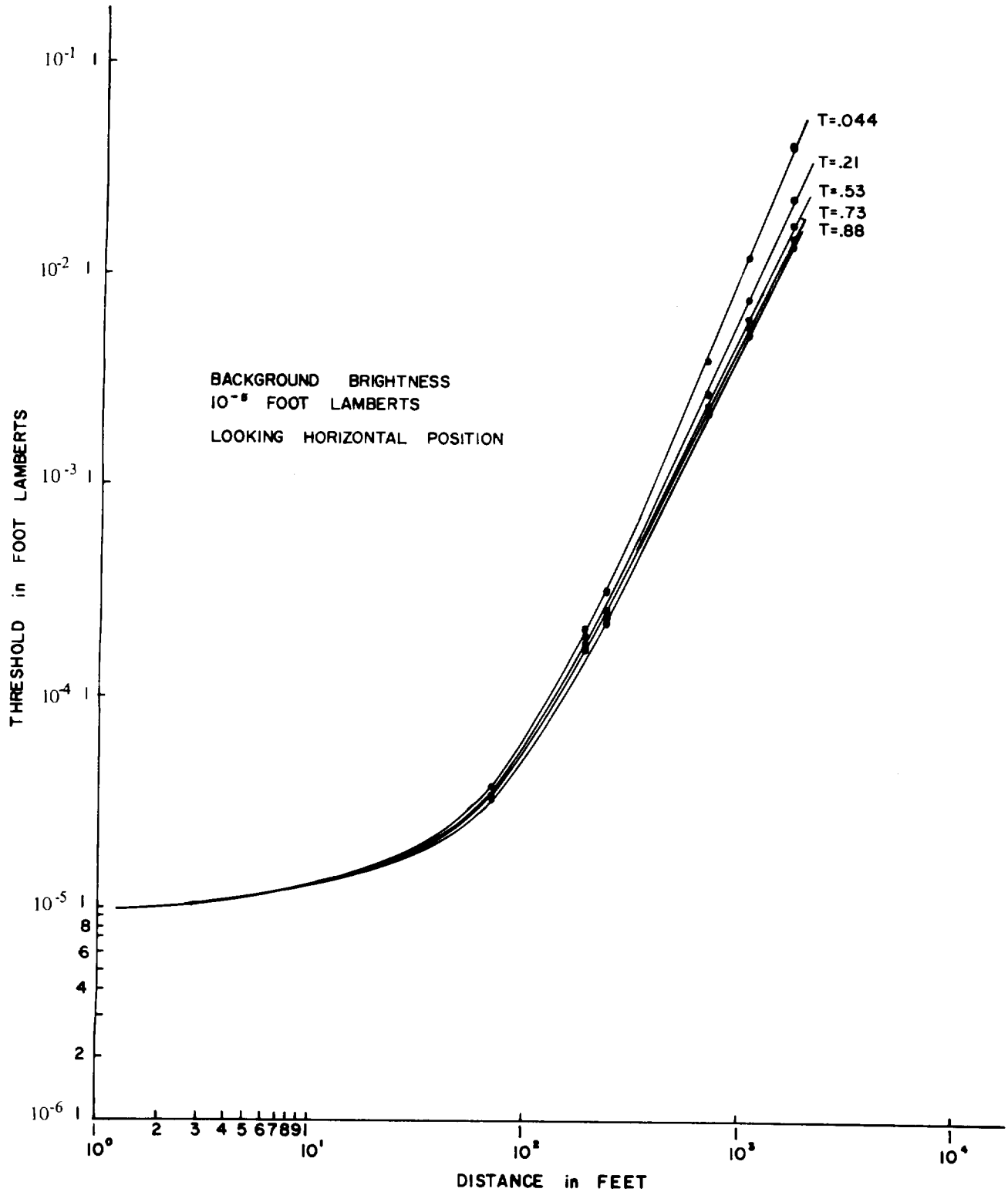

Fig. 25. RELATION BETWEEN THRESHOLD REQUIREMENTS FOR EL-PANEL (SLANT RANGE) AND DISTANCE

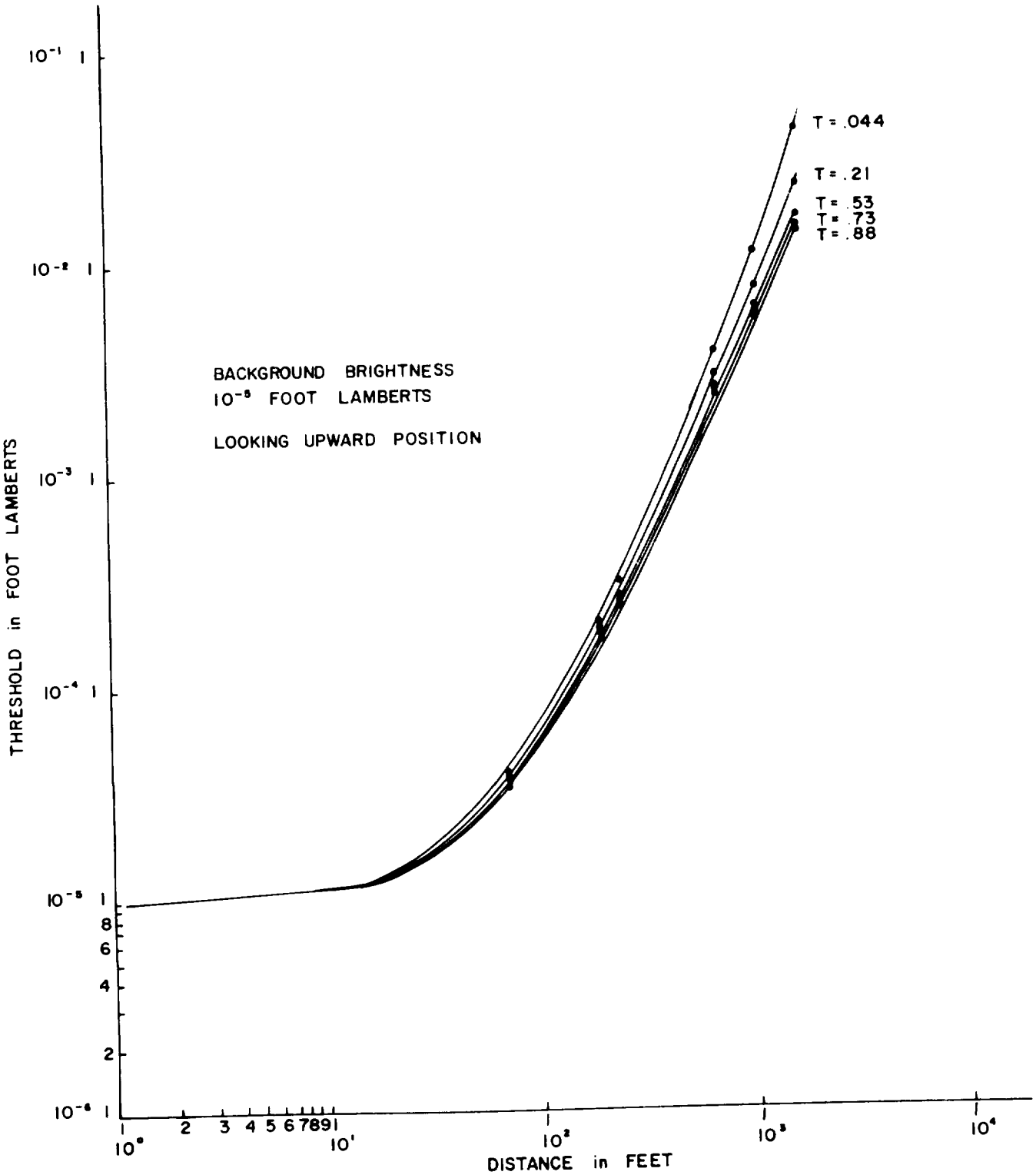

Fig. 26. RELATION BETWEEN THRESHOLD REQUIREMENTS FOR EL-PANEL (SLANT RANGE) AND DISTANCE

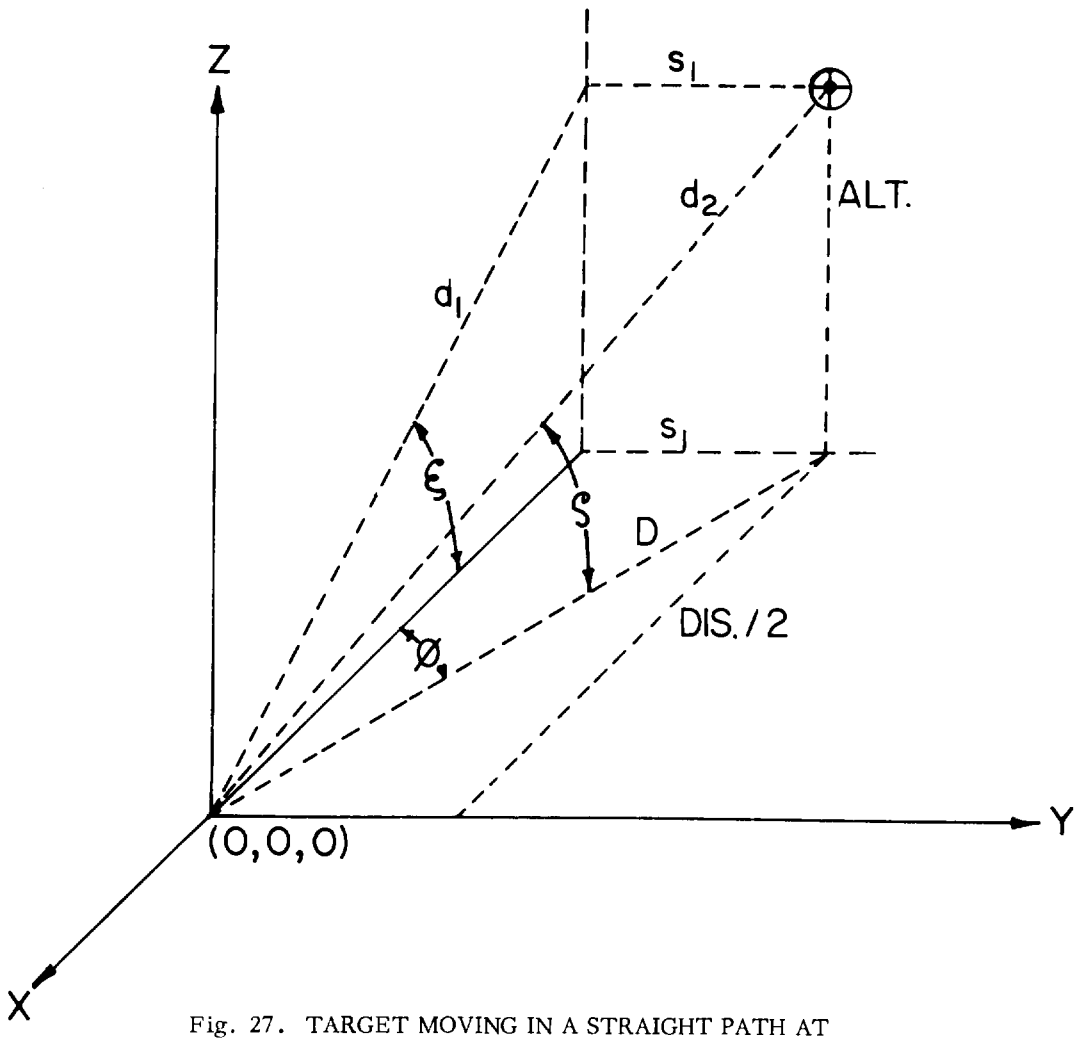

Fig. 27. TARGET MOVING IN A STRAIGHT PATH AT CONSTANT VELOCITY AND CONSTANT ALTITUDE

given: d_2, altitude and angle ϕ.

$$S_1 = d_2 \sin(\phi)$$

$$d_1 = \sqrt{(d_2)^2 - (S_1)^2}$$

$$\sin(\xi) = \frac{alt}{d_1}$$

$$\zeta = \sin^{-1}\left(\frac{alt}{d_2}\right)$$ solving for ζ we have

$$\tan(\zeta) = \frac{alt}{D}$$

$$D = \frac{alt}{\tan(\zeta)}$$ $$Dis = 2.0D\cos(\phi)$$

$$Dis = \cos(\phi) * D * 2.0$$

$$t = \frac{Dis}{V}$$ Time that target is in the Detectable Range.

duration (Bloch's Law) and that above a critical duration, t_c, the contrast $\Delta I/I$, itself, becomes constant.

Empirical results indicated that the critical time was from 0.10 to 0.0316 seconds. Probabilities of detection of 0.5 and above have been selected for analysis in this report. Furthermore, the surface light source is assumed to be a constant "on" source. Because of the range of probabilities of interest here, and because of the relatively long time required for a "look," the critical duration can be ignored in these calculations.

Hufford (7) showed that as the visual angle of the field of view increased the search time also increased. As the intensity of the light source increased, the required search time decreased. Hufford's curves showed an interesting interaction, in that if the light source increased in brightness, the search time could be held fairly constant despite an increase in field of view. If the contrast is increased greatly, e.g. by the use of extreme intensities, the effect of search area on search time may be negligle. Hence, Equation (28)

$$\Delta t = K \cdot (A)/(\Delta I/I)_L \qquad (28)$$

$$\Delta t = 0.1(A)/(\Delta I/I)_L$$

where Δt = time interval for search in seconds.

A = area of visual view in linear search (degrees)

$5 \leq A \leq 100$ (degrees)

$(\Delta I/I)_L$ = Probability level of contrast (Blackwells),

describes all of the relationships that Hufford (7) implied in his report. It has also been suggested by Lawson (1) that for each 10 degrees of linear search a delay time of approximately one second will occur. Table 6 shows the delay time (Δt) for two probability levels 0.50 and 0.95 that Hufford reported in 1964 (7). Hufford's data was obtained from two subjects viewing fields ranging from 20 to 200 minutes of visual angle. These data are shown in black in Figure 28. The suggestion by Lawson that for each 10 degrees of linear search a delay time of approximately one second will occur is also shown in dashed lines in Figure 28 for 0.50 and 0.95 detection probability.

TABLE 6

Relationship Between Area (A), Contrast $(\Delta I/I)_L$ and Delay Time (ΔT)

Δt Delay Time (Seconds)	Linear Search Area (A) (Degrees)	Contrast Probability Level	
0.3	3	1.0	(*)
1.0	10	1.0	(**)
5.0	50	1.0	(**)
7.0	70	1.0	(**)
0.4	2	0.5	(*)
1.0	5	0.5	
2.0	10	0.5	
4.0	20	0.5	

(*) agreement with Hufford's results
(**) agreement with Lawson's results

Krendel and Wodinsky (8) also investigated search in an unstructured visual field, with background luminance of 0.01, 0.1, 1.0 and 12.4 foot-lamberts. The result implied that if detection probability is to increase for a fixed light source, either the search area must decrease or the search time must increase. Further analysis shows that if Lawson's suggestion is applied, for each 10 degrees of linear search a delay time of approximately one second will occur; the width of the area of linear search must decrease if the detection probability is to increase for a fixed target (Table 7). This suggests that by increasing search time, a light source can have the same detection probability as if it were in a smaller search area. It implies that a light source must increase its intensity as the area of view becomes larger if probability of detection is to remain the same. Hence, if it takes one second to detect a light source in a search area 10 degrees square, then it will take two seconds to detect the same light source in a search area 20 degrees square. Therefore, depending upon the size of the search area, it becomes possible to set probability levels for time required for search (Fig. 29).

By using the Krendel and Wodinsky graph on required time for detection versus search area, Figure 29, it becomes possible to calculate the width of linear search. Table 7 summarizes the width that is required for 0.5 and 0.75 probability level.

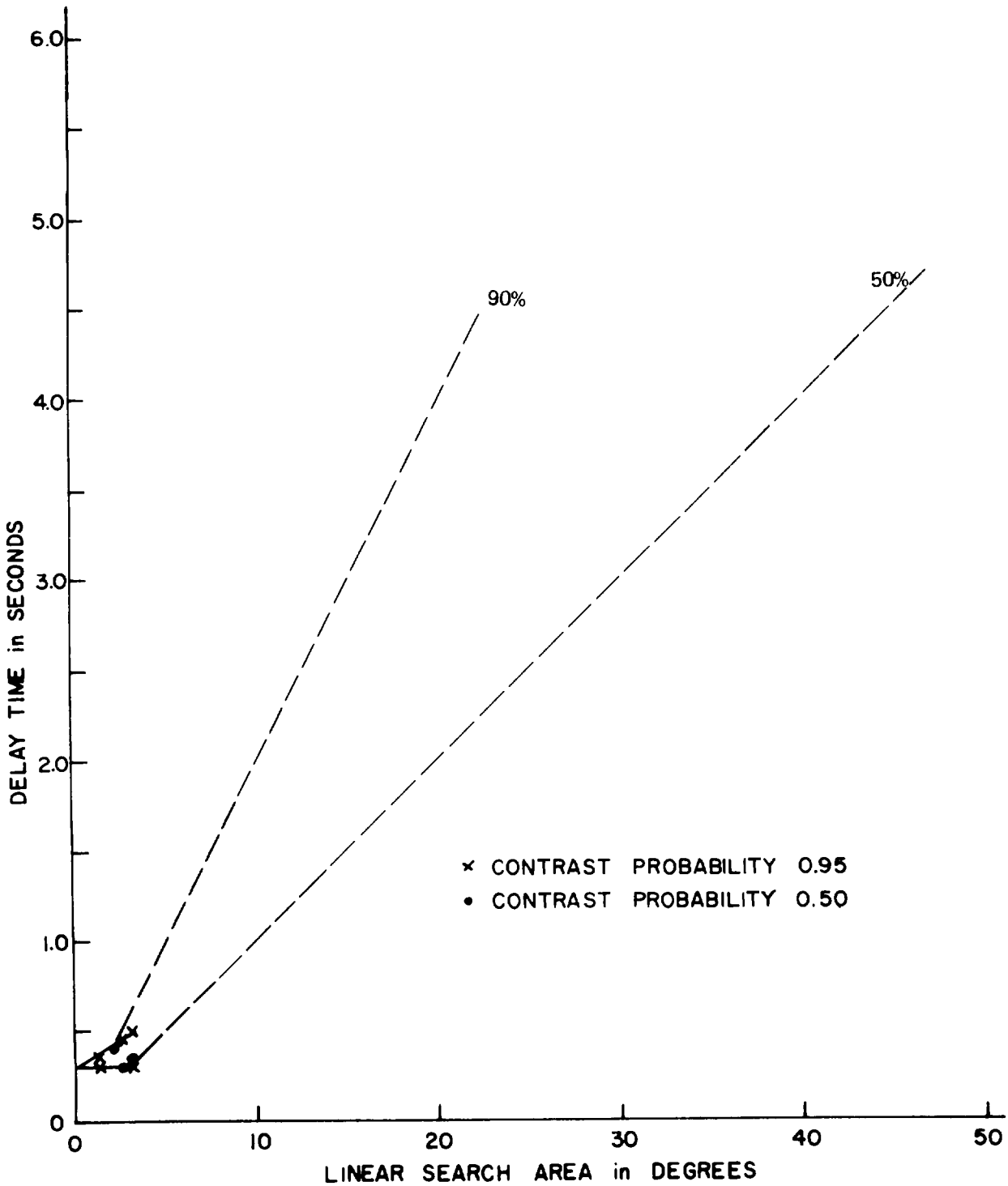

Fig. 28. RELATION BETWEEN LINEAR SEARCH AREA (A), CONTRAST ($\Delta I/I$), AND DELAY (SEARCH) TIME (Δt)

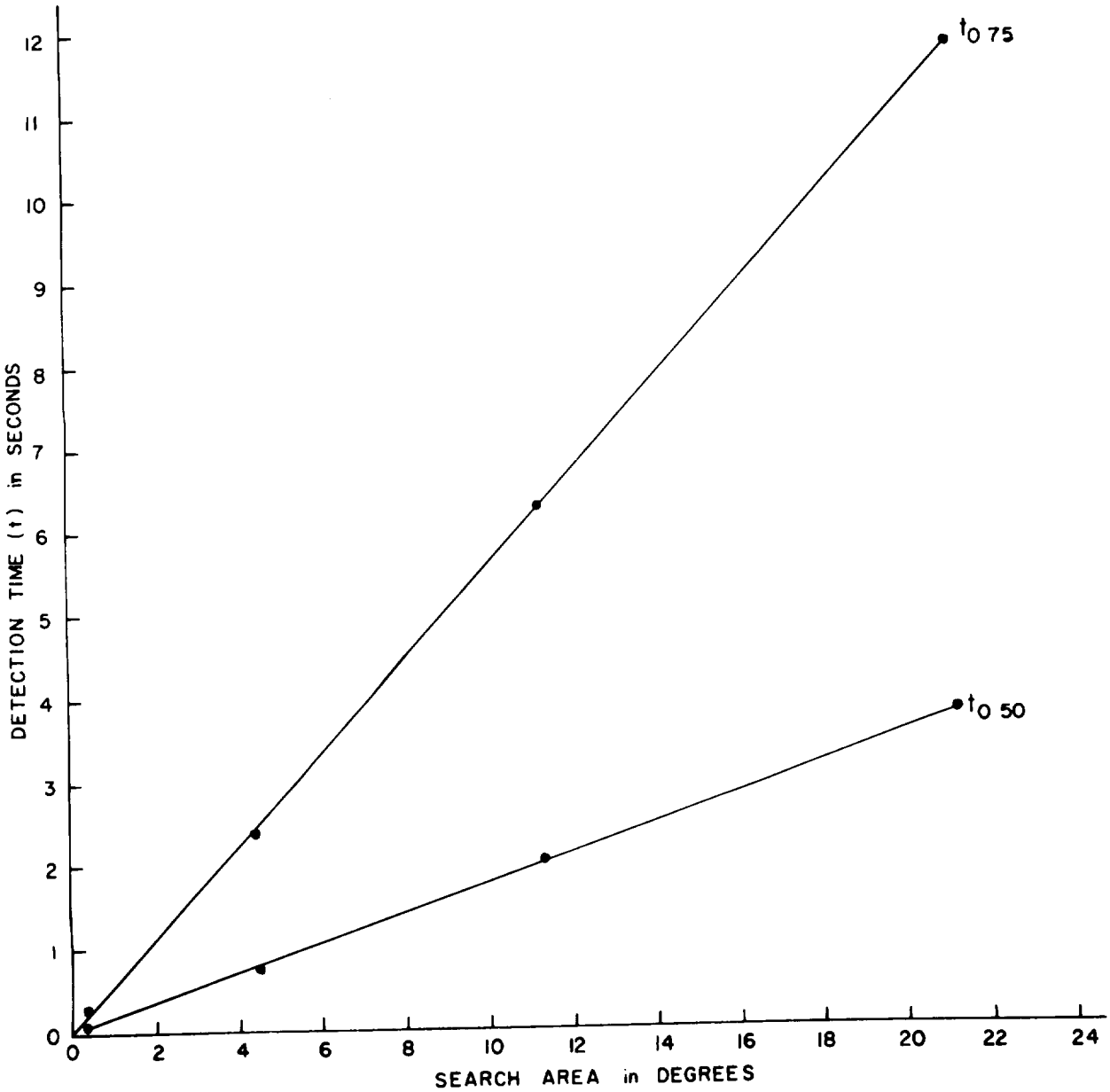

Fig. 29. TIME TO DETECTION VS SEARCH AREA; GRAND AVERAGE
(Source: Krendel & Wolinsky)

TABLE 7

Detection Probability Levels Required
for Fixed Light Sources

Area Square (Degrees)	Probability Level	Time (Seconds)	Width of the Required Search Area (Degrees)
11.244	0.5	2.0	5.622
16.867	0.5	3.0	5.6223
5.6217	0.75	3.0	1.8739
8.99	0.75	5.0	1.798
12.371	0.75	7.0	1.76728

Calculating the width of the required linear search area shows that the width is a constant for 0.5 and 0.75 probability.

Since, for every second that the observer is exposed to the target, the target will either increase or decrease in size, and hence the probability of detection will also increase or decrease depending upon the conditions. It becomes essential that the probability levels be known for a fixed target. Equations (20), (23) and (24) from the previous section on attenuation and scatter compute the inherent contrast of a fixed target at a given distance required for detection. For example, the 10 x 2 inch EL. panel will have a probability level of 0.50 at a distance of 1,063 feet with background brightness 1.0×10^{-5} foot-lamberts if the surface target brightness level is 4.94×10^{-3} foot-lamberts. This brightness was computed by using Equation (23) for the upward case. Since the background brightness is so small and the brightness level is known (4.94×10^{-3} foot-lamberts), we can calculate the 0.60, 0.70, 0.80, etc., detection requirements for the EL. panel (Table 8). Definition of contrast ratio:

$$\frac{B_S - B_O}{B_O} = C$$

where B_O is small and equal to ϵ for low background luminance.

Therefore, $B_S = C\epsilon + \epsilon$

in this particular case the contrast ratio is:

$$\frac{.004936 - .00001}{.00001} = 492.6$$

Since the relative contrast for 0.50 probability level is 4.92.6, we know that by increasing the contrast level to 798.12 (or by a factor of 1.62 using Blackwell's relative contrast curve (Fig. 30) we can increase the probability of detection to 0.90. This idea can be applied from another point of view. At what distance will the EL. panel with 4.94×10^{-3} foot-lamberts brightness have 1.62 more contrast brightness $(\Delta I/I)_t$ than the required 0.50 threshold level? This can be solved since the size is already taken into consideration, by dividing contrast by 1.62. We are essentially dividing $B_s = 4.936 \times 10^{-3}$ by 1.62. Since B_o (background brightness) is so small, and equal to ϵ:

$$\frac{4.936 \times 10^{-3}}{1.62} = 3.04691 \times 10^{-3} \text{ foot-lamberts}$$

The threshold brightness in the curves (Fig. 31) shows that this corresponds to a distance of 820.0 feet. Rechecking the calculation:

$$\frac{.0030469 - .00001}{.00001} = 303.69$$

The required 0.50 probability level at 820 is 3.0469×10^{-3} foot-lamberts.

Therefore, the EL. panel with 4.936×10^{-3} foot-lamberts brightness will be 0.90 detectable at a range of 820.0 feet.

$$\frac{.004936 - .00001}{.00001} = 492.6 = (303.69)(1.62)$$

The required 0.90 probability level at 820 feet is 4.936×10^{-3} foot-lamberts.

The curves in Figure 30 show that for small background brightnesses this method of calculating probability levels is accurate. Table 8 gives the probability levels for the case just considered, and Figure 31 gives a graphical presentation of case.

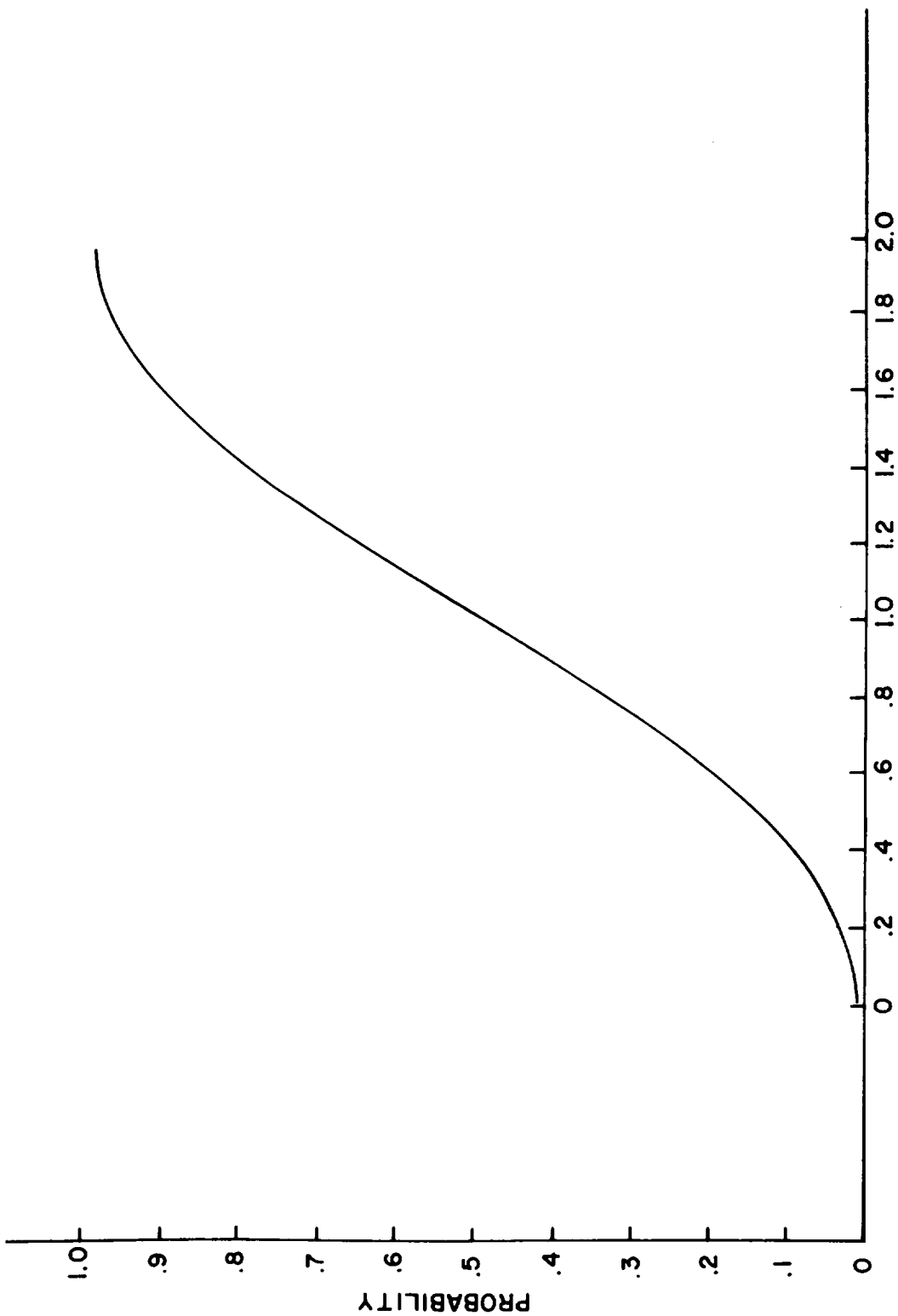

Fig. 30. AVERAGE PROBABILITY CURVE FOR 450,000 SAMPLE POPULATION

TABLE 8

Probability Levels for an Approaching Target of
$.4936 \times 10^{-2}$ Foot-Lamberts at 1,063 Feet

Brightness of Target	0.5 Probability Level of EL. Panel (Foot-Lamberts)	Probability + Contrast Factor	Distance From Observer (Feet)	Elapsed Time (Seconds)
4.93×10^{-3}	1.234×10^{-2}	0.10 (0.40)	1,700	0.0
4.93×10^{-3}	$.8226 \times 10^{-2}$	0.20 (0.60)	1,400	2.205
4.93×10^{-3}	$.67616 \times 10^{-2}$	0.30 (0.73)	1,260	3.235
4.93×10^{-3}	$.57395 \times 10^{-2}$	0.40 (0.86)	1,160	3.970
4.93×10^{-3}	$.4936 \times 10^{-2}$	0.50 (1.0)	1,063	4.684
4.93×10^{-3}	$.429217 \times 10^{-2}$	0.60 (1.15)	1,010	5.074
4.93×10^{-3}	$.37969 \times 10^{-2}$	0.70 (1.30)	930	5.662
4.93×10^{-3}	$.34517 \times 10^{-2}$	0.80 (1.43)	900	5.882
4.93×10^{-3}	$.30469 \times 10^{-2}$	0.90 (1.62)	820	6.471
4.93×10^{-3}	$.263957 \times 10^{-2}$	0.95 (1.87)	770	6.838
4.93×10^{-3}	$.2468 \times 10^{-2}$	0.99 (2.0)	740	7.059

Velocity 136 ft/sec.
Transmittance per mile looking upward with T = .88 10^{-5} foot-lamberts

Let us assume that the observer is searching, in a linear search area of 10 degrees. What is the probability that detection will be accomplished by the time the target is 900.0 feet from the aircraft, if the 10 x 2 inch EL. panel has 4.94×10^{-3} foot-lamberts brightness in a 10^{-5} foot-lamberts background?

By use of Equation (28), it is possible to compute the time needed for detection if detection is to occur. Table 9 gives a summary of the computations, starting at 0.50 probability level. The probability rule that relates the time duration with the level of detection is given below:

$$\Delta t = 0.1\,(10.)_{/0.50} = 2.0 \text{ sec.} \quad (\pm 1.0)$$

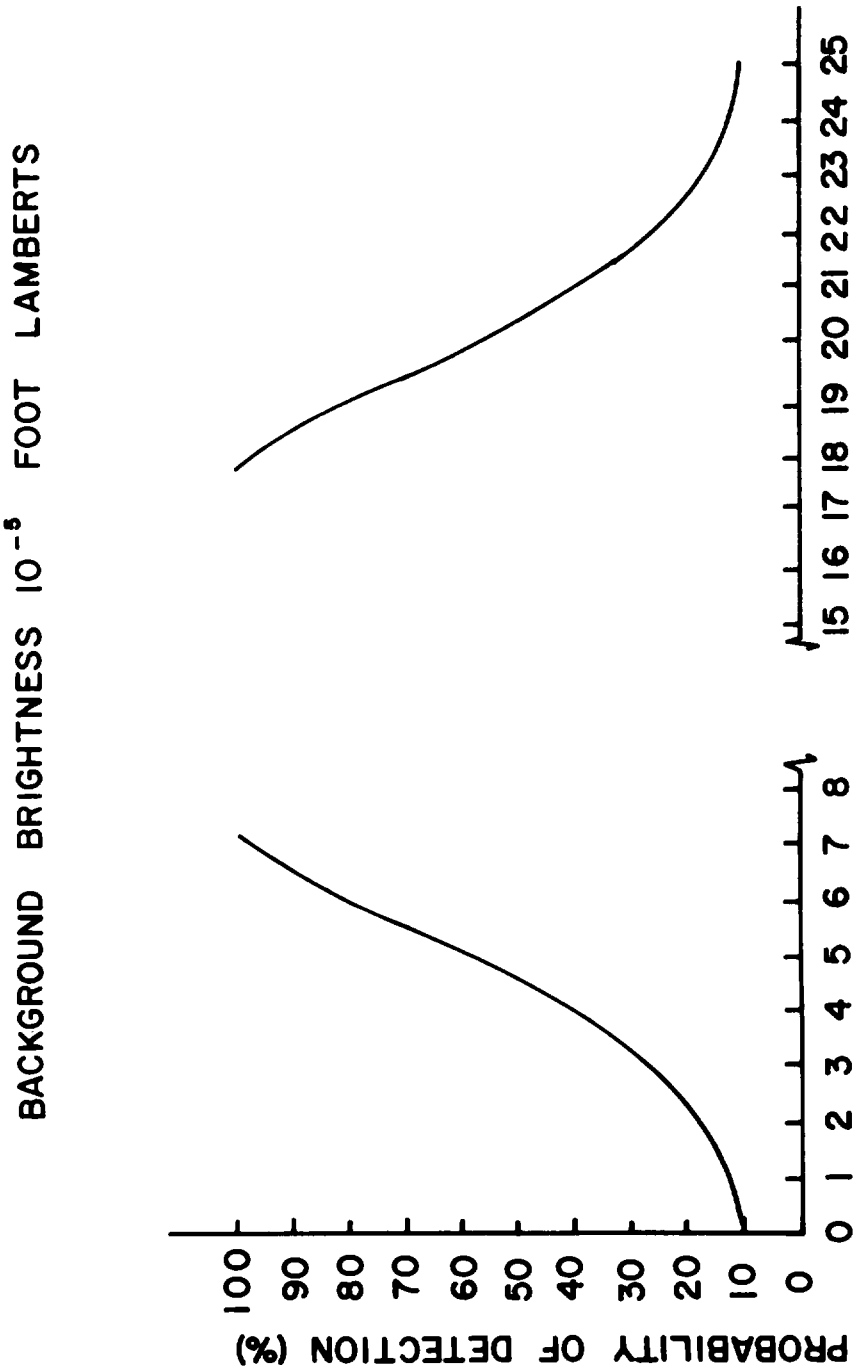

Fig. 31. DETECTION PROBABILITY FOR EL-PANEL WITH BRIGHTNESS 4.936×10^{-3}

TABLE 9

Time Required to Detect the Approaching Target in Figure 15

$\left(\Delta I/I\right)_L$	Time Above and Below	Area (Degrees)	Δt_B (Seconds)
0.50	$\pm$ 1.0	10.0	2.0
0.70	$\pm$ 0.714	10.0	1.428
0.88	$\pm$ 0.568	10.0	1.1363

It takes two (2.0) seconds to search a linear area of 10^{o}; one (1.0) second above and below the 0.50 probability level. After a time interval of (+1) one second on the x-axis, the target is now at the detectable level of 0.70, computing the time required for detection at 0.70 probability level, which is 1.428 seconds. This means that 0.714 seconds will be distributed above the 0.70 probability level. Displacing the 0.70 probability level by 0.714 second, we reach the 0.88 probability level (Table 9) of detection.

$$t = 0.1\,(10.)_{/(0.70)} = 1.428$$

The mathematics to associate Table 9 with the probability rules is given below:

Let $P_1 = \epsilon_1$ the probability of detection on first look.

$\bar{P}_1 = 1 - \epsilon_1$ the probability of no detection on first look.

$P_2 = \epsilon_2$ the probability of detection on second look.

$\bar{P}_2 = 1 - \epsilon_2$ the probability of no detection on second look.

.
.
.

$P_n = \epsilon_n$ the probability of detection on nth look.

Hence, the probability that the target will be detected by time it gets to within 900 feet of the observer is:

$$P_1 = \epsilon_1$$

$$P_{1+2} = \epsilon_1 + (1-\epsilon_1)(\epsilon_2) = P_1 + (1-P_1)\epsilon_2$$

$$P_{1+2+3} = \epsilon_1 + (1-\epsilon_1)(\epsilon_2) + 1-(\epsilon_1+(1-\epsilon_1)\epsilon_2)\ \epsilon_3$$

$$= P_{1+2} + (1-P_{1+2})\ \epsilon_3$$

$$P_{1+2+\ldots n} = \epsilon_1 + (1-\epsilon_1)\ \epsilon_2 + \ldots\ldots + 1-(\epsilon_1+(1-\epsilon_1)\epsilon_2 +$$

$$(1-(\epsilon_1+(1-\epsilon_1)\ \epsilon_2)\epsilon_3 + \ldots = P_{.1+\ldots+n-1})\ \epsilon_n$$

Assuming that the first look is at threshold (0.50) brightness and the second look is at 0.70 probability of detection level.

$$P(\text{detection}) = \epsilon_1 + (1.-\epsilon_1)(\epsilon_2)$$

$$= 0.5 + (1.-0.5)(0.7)$$

$$= 0.5 + (0.5)(0.7)$$

$$= 0.5 + 0.35$$

$$P(\text{detection}) = 0.85 = 85\% \quad \text{at 900 feet from target.}$$

The probability can also be calculated for an example where three searches are required to detect the target:

EXAMPLE:

$$P_1 = \epsilon_1 = .5$$

$$P_2 = \epsilon_2 = .7$$

$$P_3 = \epsilon_3 = .8$$

$$P_{1+2+3} = (.5) + (1-.5)(.7) + (1-(.5+(.5)(.7)(.8)$$

$$= 0.5 + (.5)(.7) + (1-.83)(.8)$$

$$= 0.3 + 0.35 + (0.15)(.8)$$

$$= 0.5 + 0.35 + .120$$

$$= 0.97$$

Therefore, the longer the length of run the higher the probability of detection. It is also apparent that the larger the area of search the lower the probability of detection. Thus, we have one method of approximating the integral under the probability curve and considering both the length of time in view and the area of search.

SUMMARY

The analysis of visibility of a surface light must bring all the individual factors together. The first consideration must be given to the surface light itself, the shape and relative size in square minutes of arc. If the shape of the target does not approximate a circle on square in form, then the contrast threshold can be computed by Lamar's useful flux method.

$$\left(\Delta I/_I\right)_t = CR^k/A_1$$

This computation is shown in section (b) of this report using Hardy's data on contrast ratios for different subtended minutes of visual arc.

After the contrast threshold levels have been computed for variable shapes and sizes, apparent contrast (C_A), this input data is used to calculate the needed inherent contrast requirements (C_o) for the variable conditions. Some of the conditions to be considered are: (a) attenuation and scatter, (b) slant range, (c) sky-ground ratios and (d) relative number of particles per unit volume atmosphere. The equations used for this computation are (20), (23) and (24) by Duntley.

Now that the brightness levels for target detection are determined, further predictions directly related to the unique environmental conditions for each case must be investigated. How long will the target be in the visible range? How large will the search area be? Search time (Δt) in relation to search area can be associated using the equation:

$$\Delta t = k(A)/\left(\Delta I/_I\right)_L \qquad (28)$$

thereby determining the cumulative probability of detection for a particular case. Accuracy in integration of the area under the cumulative probability curve can be increased by the use of appropriate weights, which, in effect, narrow the width of the search time segments and smooth the detection probability approximations. Thus, it becomes possible to associate a probability value with each case. This analysis for a given surface light source can give a reasonably accurate prediction of detection probability.

REFERENCES

1. Ballantyne, F. P. Initial technical guidance for visionics contract (Report of 6 May, Visit of NVL), 2147.3/456, Hughes Aircraft Company IDC, 8 May 1968.

2. Blackwell, H. R. Contrast threshold of the human eye. Journal of the Optical Society of America, 1946, 36, 624-643.

3. Brown, R. H. The upper speed threshold for the discrimination of velocity as a function of stimulus luminance. NRL Report 4862, November 1956.

4. Duntley, S. Q. The reduction of apparent contrast by the atmosphere. Journal of the Optical Society of America, 1948, 38, 179-191.

5. Graham, C. H., & Kemp, E. H. Brightness discrimination on a function of the duration of the increment in intensity. Journal of General Physiology, 1938, 21, 635-650.

6. Hardy, C. A. Visibility data and the use of optical aids. E-1385, Massachusetts Institute of Technology, Cambridge, Mass., July 1963.

7. Hufford, L. E. Reaction time and the retinal area - stimulus intensity relationship. Journal of the Optical Society of America, 1964, 54, 1368-1373.

8. Krendal, E. S., & Wodinsky, J. Search in an unstructured visual field. Journal of the Optical Society of America, 1960, 50, 562-568.

9. Lamar, E. S., Hecht, S., Hendley, C. D., & Shlaer, S. Size, shape and contrast in detection of targets by daylight vision. II. Frequency of seeing and the quantuum theory of cone vision. Journal of the Optical Society of America, 1948, 38, 741-755.

APPENDIX A

PROGRAM TO COMPUTE LIGHT REQUIREMENTS FOR TARGET DETECTION

A computer program was written to incorporate and interrelate the factors developed in this study. The flow chart (Fig. 1A) illustrates the relationships among factors developed in the previous sections.

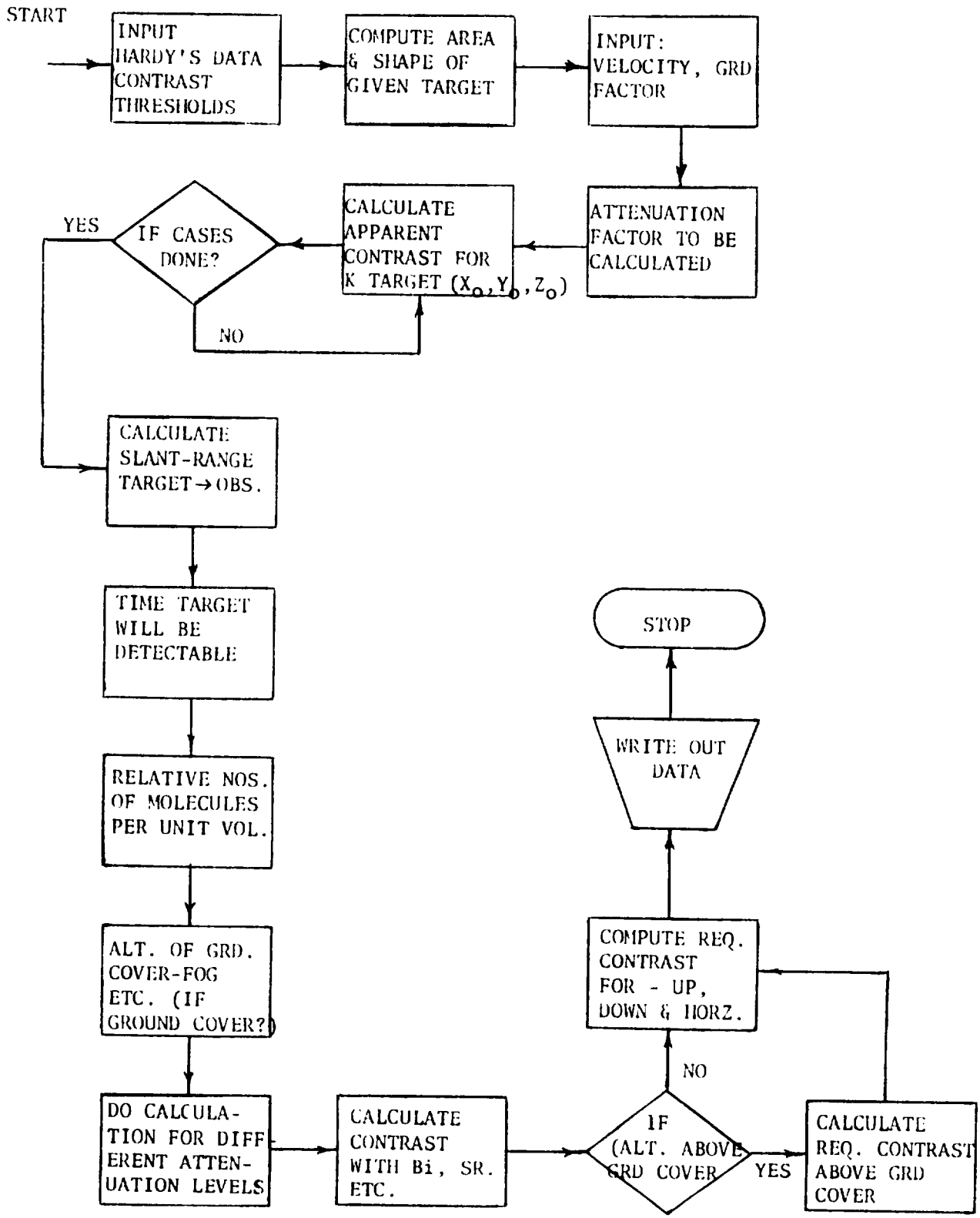

Fig. 1A. FLOW CHART FOR COMPUTER PROGRAM

DISTRIBUTION LIST

CG, USAMC, Wash, D. C.
- AMCRDL (Ofc of Dep for Labs) 1
- AMCRD (Air Def & Msl Ofc) 1
- AMCRD (Air Mobility Ofc) 1
- AMCRD (Comm-Elec Ofc) 1
- AMCRD G 1
- AMCRD (Weapons Ofc) 1
- AMCRD (Dr. Kaufman) 1
- AMCRD (Mr. Crellin) 1

Ofc of Chief of Staff, DA, Wash, D. C.
- CSAVCS W TIS 1

USA Behavioral Science Rsch Lab.
Arlington, Va. 1

Dr. J. C. Uhlaner, Dir.
USA Behavioral Science Rsch Lab.
Arlington, Va. 1

Behavioral Sciences Division
Ofc, Chief of Rsch & Development, DA
Washington, D. C. 1

Deputy Chief of Staff for Personnel
Dept of Army, Wash, D. C.
- Personnel Rsch Div. 1

CG, USACDC, Fort Belvoir, Va.
- CDCCD-C 1
- CDCMR 1
- CDCRE 1

CO, USACDC Air Defense Agency
Fort Bliss, Texas 1

CO, USACDC Armor Agency
Fort Knox, Ky. 1

CO, USACDC Artillery Agency
Fort Sill, Okla. 1

CO, USACDC Aviation Agency
Fort Rucker, Alabama 1

CO, USACDC CBR Agency
Fort McClellan, Alabama 1

CG, USACDC Combat Arms Group
Fort Leavenworth, Kansas 1

CG, USACDC Combat Svc Spt Gp.
Fort Lee, Va. 1

CO, USACDC Comm-Elec Agency
Fort Monmouth, N. J. 1

CO, USACDC Engineer Agency
Fort Belvoir, Va. 1

CO, USACDC Inst of Strat & Stab Opns
Fort Bragg, N. C. 1

CO, USACDC Med Svc Agency
Fort Sam Houston, Texas 1

CO, USACDC Military Police Agency
Fort Gordon, Georgia 1

CO, USACDC Supply Agency
Fort Lee, Va. 1

USACDC Experimentation Command
Fort Ord, Calif.
- Liaison Office 1
- Tech Library, Box 22 1

Human Factors Division
G-2/3, USACDCEC
Fort Ord, Calif. 1

CO, USA Environ Hygiene Agency
Edgewood Arsenal, Md.
- Librarian, Bldg 2400 2

Human Factors Br, Med Rsch Lab
Rsch Labs, Edgewood Ars, Md. 1

CO, USA Edgewood Arsenal
- Psychology Branch 1

CO, Frankfort Arsenal, Phila. Pa.
- SMUFA-N/6400/202-4 (HF) 1
- Library (C2500, B1 51-2) 1

CO, Picatinny Arsenal, Dover, N. J.
- SMUPA-VC1 (Dr. Strauss) 1

CG, USA Electronics Command
Fort Monmouth, N. J.
- AMSEL-RD-GDA 1

Dir, Military Psychol & Leadership
US Mil Academy, West Point, NY 1

CO, Watervliet Arsenal, N. Y.
- SWEWV-RDT 1

CO, USA Med Equip Rsch & Dev Lab
Fort Totten, Flushing, LI, NY 1

CO, USA Rsch Inst of Envir Med
Natick, Mass.
- MEDRI-CL (Dr. Dusek) 1

CG, USA Medical R&D Command
Main Navy Bldg, Wash, D.C.
- Behavioral Sciences Rsch Br 1

Dir, Walter Reed Army Inst Rsch
Washington, D. C.
- Neuropsychiatry Div. 1

CO, Harry Diamond Laboratories
Washington, D. C.
- AMXDO-EDC (B. I. Green) 1

CO, USA Mobility Equip R&D Ctr
Fort Belvoir, Va.
- Human Factors Engr. 1

USAETL-TEB
Fort Belvoir, Va.
- T. L. Fick 1

U. S. Army Natick Laboratories
Natick, Mass.
- AMSRE-STL
- Tech Library 1

Commandant, Army Logistics
Mgmt Ctr, Fort Lee, Va.
- E. F. Neff, Proc Div. 1

USA Gen Equip Test Activity
Methods Engr Dir, Hum Fact Div
Fort Lee, Va. 1

CG, US CONARC
Fort Monroe, Va. 1
- ATIT RD-RD 1

CO, USA Rsch Ofc, Box CM
Duke Station, Durham, N. C. 1

Dir Rsch, USA Avn HRU
PO Box 428, Fort Rucker, Ala.
- Librarian 1

CG, USA Missile Command
Redstone Arsenal, Ala.
- AMSMI-RBLD 1
- AMSMI-RSB (Chaikin) 1

President, USA Infantry Board
Fort Benning, Georgia 1

President, USA Maintenance Board
Fort Knox, Ky.
- Adjutant 1

USA Armor, Human Rsch Unit
Fort Knox, Ky.
- Library 1

CO, USA Med Rsch Lab
Fort Knox, Ky. 1

CG, USA Weapons Command
Rock Island, Ill.
- AMSWE-RDT 1
- AMSWE-SMM-P 1
- SWERI-RDD-PD 2

CG, USA Tank-Automotive Command
Warren, Michigan
- SMOTA-RR 1
- AMSTA-BSL 2
- AMSTA-BAE 1

Director of Research
Hum RRO Div. No. 5 (Air Defense)
PO Box 6021, Fort Bliss, Texas 1

Commandant, USA Artillery & Missile School, Fort Sill, Okla.
USAAMS Tech Library 1

CG, White Sands Msl Range, NM
Technical Library 1
STEWS-TE-Q (Mr. Courtney) 1

CG, USA Elec Proving Ground
Fort Huachuca, Ariz.
Mr. Abraham, Test Dir. 1

CO, Ft Huachuca Spt Comd, USA
Fort Huachuca, Ariz.
Tech Ref Div 1

CO, Yuma Proving Ground
Yuma, Ariz.
Technical Library 1

CO, USA Tropic Test Center
PO Drwr 942, Fort Clayton, CZ
Behavioral Scientist 2

CO, USA Arctic Test Center
APO Seattle, Wash.
STEAC-IT 1

USA Test & Eval Command
Bldg 3071, APG 1

USACDC Liaison Office
Bldg 3071, APG 1

CO, USACDC Maint Agency
Bldg 305, APG 1

Tech Libr, Bldg 3002, APG 1

Dir, Naval Research Laboratory
Washington, D. C.
Code 5120 1
Code 5143A 1

Code 455 Ofc of Naval Research
Washington, D. C. 2
Engr Psychol (Dr. Tolcott) 1

Dr. Morgan Upton
Aerospace Med Rsch Dept
US Naval Air Dev Ctr
Johnsville, Pa. 1

USN Submarine Med Ctr, Libr
Box 600, USN Sub Base
Groton, Conn. 1

CO & Dir, Naval Training Dev Ctr.
Orlando, Fla.
Technical Library 1

US Navy Electronics Laboratory
San Diego, Calif.
Ch, Human Factors Div. 1

US Marine Liaison Ofc, Bldg 3071 1

RADC (EMEDI)
Griffiss AFB, N. Y. 1

Hq, ESD (ESTI)
L. G. Hanscom Field
Bedford, Mass. 1

Wright Patterson AFB, Ohio
6570 AMRL (MRHE) 2
6570 AMRL (MRHER/Bates) 1
6570 AMRL (MRHE/Warrick) 1
Air Force Flight Dynam Lab 1

AMD (AMRH) Brooks AFB, Tex. 1

Civil Aeromedical Institute
Fed Avn Agency Aero Center
PO Box 25082, Okla City, Okla.
Psychol Br, AC 118 1

USPO Dept, Bur Rsch & Engr, HF Br.
Washington, D. C.
Mr. D. Cornog 1

US Dept Commerce, CFSTI
Sills Bldg, Springfield, Va. 2

Defense Documentation Center
Cameron Station, Alexander, Va. 20

Library, George Washington Univ.
Hum RRO, Alexandria, Va. 1

Amer Inst for Research
8555 16th St., Silver Spring, Md.
Library 1

Amer Inst for Research
135 North Bellefield, Pgh., Pa.
Library 1

Amer Inst for Research
PO Box 1113, Palo Alto, Calif.
Library 1

Ctr for Research in Social Systems
The American University
Washington, D. C. 1

The Franklin Inst Research Labs.
Phila, Pa.
Tech Reports Library 1

Inst for Defense Analyses
Arlington, Va.
Dr. J. Orlansky 1

Serials Unit, Purdue University
Lafayette, Ind. 1

Code 458 Ofc of Naval Research
Washington, D. C.
Pers & Trng (Dr. Farr) 1

Dept Psychol, Univ of Maryland
College Park, Md. 1

Mr. R. K. Brome, Govt Pub Section
JFK Memorial Library
Calif State College Los Angeles
Los Angeles, Calif. 1

Dr. R. G. Pearson, Dept of Ind Eng
North Carolina State Univ.
Raleigh, N. C. 1

Dr. F. Loren Smith
Dept Psychol, Univ Delaware
Newark, Del. 2

Dr. H. W. Stoudt
Harvard Univ., Boston, Mass. 1

Dr. Leonard Uhr
Computer Sci Dept, Univ Wisconsin
Madison, Wisc. 1

Dr. R. A. Wunderlich
Psychol Dept, Catholic Univ.
Washington, D. C. 1

Psychological Abstracts
1200 17th Street, NW
Washington, D. C. 1

AC Electronics Div, GMC
Milwaukee, Wisc.
J. S. Inserra, HF 1
Tech Library, Dept 32-55 2A 1

Libr, Chrysler Def Engr, Detroit 1

Grumman Aircraft Engr Corp.
Bethpage, LI, NY
L. Bricker, Life Sci, Plant 5 1

Hughes Aircraft Co, Culver City, Calif.
Co. Tech. Doc. Ctr. E/110 1

Itek Corp, Lexington, Mass. 1

Mgr, Behavioral Sciences, Litton Sci Spt
Lab, Fort Ord, Calif. 1

U. S. Army Natick Laboratories
Natick, Mass.
AMXRE-PRB 1
AMXRE-PRBN 1
AMXRE-PRBE 1

USA Bd for Avn Accident Rsch Lab
Fort Rucker, Ala
Gail Binkston, Bldg 5504 1

Federal Aviation Administration
800 Independence Ave, S.W.
Washington, D. C.
Admin Stds Div (MS-110) 1

Dr. Lauritz S. Larsen
Automobile Manufacturers Assoc.
320 New Center Building
Detroit, Mich. 1

Dr. Irwin Pollack
University of Michigan
Ann Arbor, Mich. 1

Dr. Harvey A. Taub
Rsch Sec, Psychology Service
VA Hospital, Irving Ave & Univ Pl
Syracuse, New York 1

Documents Librarian
Wilson Library
University of Minnesota
Minneapolis, Minn. 1

Research Analysis Corporation
McLean, Va.
Document Library 1

Ritchie, Inc.
Dayton, Ohio 1

Director, Human Factors Engr
Mil Veh Org, GMC Tech Center
Warren, Mich. 1

Sprint Human Factors MP 537
Martin Co., Orlando, Florida 1

Dr. Herbert J. Bauer
GM Rsch Labs, GM Tech Center
Warren, Mich. 1

Dr. Edwin Cohen
Link Group, Gen Precision Sys Inc.
Binghamton, New York 1

Mr. Henry E. Guttmann
Sandia Corporation
Albuquerque, New Mexico 1

Dr. M. I. Kurke
Human Sciences Rsch Inc.
McLean, Virginia 1

Mr. James Moreland
Westinghouse Elec Corp, R&D Ctr
Churchill Boro
Pittsburgh, Pa. 1

Mr. F. M. McIntyre, HF Engr
Cleveland Army Tank-Auto Plant
Cleveland, Ohio 1

Mr. Robert F. Roser, HF Sys Engr
General Dynamics Pomona
Box 2507
Pomona, Calif. 1

Dr. S. Seidenstein, Org 55-60
Bldg 151, Lockheed, P.O. Box 504
Sunnyvale, Calif. 1

Mr. Wesley E. Woodson
MAN Factors, Inc.
San Diego, Calif. 1

Mr. C. E. Righter
Airesearch Mfg Co
Los Angeles, Calif. 1

Dr. Charles Abrams
Human Factors Research
Goleta, Calif. 1

Mr. Wardell B. Welch
Code 3400
Naval Electronics Lab Center
San Diego, Calif. 1

Dr. Corwin A. Bennett
Kansas State University
Manhattan, Kansas 1

The University of Wyoming
Laramie, Wyoming
Documents Library 1

Dr. Lawrence C. Perlmuter
Bowdoin College
Brunswick, Maine 1

Dr. Alexis M. Anikeeff
The University of Akron
Akron, Ohio 1

CG, USASCOM
P.O. Box 209
St. Louis, Missouri
AMSAV-R-F (S. Moreland) 1

Dr. Arthur Rubin
U. S. Dept of Commerce
National Bureau of Standards
Washington, D. C. 1

The Boeing Co., Vertol Div.
Philadelphia, Pa
Mr. Walter Jablonski 1

Mr. Gerald J. Fox
Grumman Aerospace Corp.
Bethpage, New York 1

BioTechnology, Inc.
Falls Church, Virginia
Librarian 1

Prof. Richard C. Dubes
Michigan State University
East Lansing, Mich. 1

Dr. Bill R. Brown
University of Louisville
Louisville, Kentucky 1

Prof. James K. Arima
Dept of Operations Analysis
Naval Postgraduate School
Monterey, Calif. 1

COL Roy A. Highsmith, MC
Hq, USATECOM, APG
AMSTE-SS 1